Project File Number	OU 7-06
EDF Serial Number	ER-WAG7-54
Functional File Number	
INEL Report Number	INEL-94/064

ENGINEERING DESIGN FILE

Project/Task _____

Subtask _____ **EDF Page** 1 **of** 41

Title: Results from the Large-Scale Aquifer Pumping and Infiltration Test Down-Hole Gamma Spectroscopic Monitoring

Summary:

The summary briefly defines the problem or activity to be addressed in the EDF, gives a summary of the activities performed in addressing the problem and states the conclusions, recommendations, or results arrived at from this task.

This EDF provides a summary of the data obtained by the gamma spectroscopy monitoring system used in support of the Aquifer Pumping and Infiltration Test. Gamma spectroscopy data obtained during the test have been reviewed and the most relevant data incorporated into this report.

Distribution (complete package): Kirk Dooley (3920), Gary Mecham (3939)

Distribution (summary page only):

Author: Dept.	Reviewed: Date	Approved Date
F. M. Dunnivant Int. Earth Sci. G. D. Mecham Env. Restoration J. Giles 1/17/95		G.J. Stanley 1/24/95
	LITCO Review Date Jerry P. Sloan JAN 17, 95	LITCO Approval Date Kirk J. Dooley 1/17/95

CONTENTS

Results from the Large-Scale Aquifer Pumping and Infiltration Test Down-Hole Gamma Spectroscopy Monitoring

INTRODUCTION

The purpose of this Engineering Design File (EDF) is to summarize the data obtained by the gamma spectroscopy monitoring system used in support of the Aquifer Pumping and Infiltration Test. Gamma spectroscopy data obtained during the test have been reviewed and the most relevant data sets are summarized here. Gamma spectroscopic data were used for radionuclide (tracer) identification, both qualitatively and quantitatively, by identifying characteristic peaks produced by gamma ray emission from the tracers. Figure 1 shows a typical gamma ray spectrum. The data files are often referred to as spectrum files. These data include the monitoring of the basin water during tracer introduction, monitoring of saturated zones in B and C wells, and monitoring of five wells located inside the infiltration basin. All of the data collected during the test will be maintained at the Idaho National Engineering Laboratory (INEL) Administrative Record and Document Control (ARDC).

The main objective for using down-hole gamma spectrometry, as described in the test plan (EGG-ER-11364), was to obtain tracer breakthrough curves (BTCs) in unsaturated zones or zones where water samples were unavailable in the subsurface. As the test evolved, the system was also used for determining the integrity of monitoring well installation inside the basin, evaluating the vertical distribution of tracers in unsaturated and saturated zones, and surveying for surface contamination after the violent wind storm on July 31, 1994.

SYSTEM DESCRIPTION

Two down-hole gamma spectroscopy systems were utilized during the Aquifer Pumping and Infiltration Test: (1) the Radionuclide Logging System (RLS) from Westinghouse Hanford Company, and (2) the Gamma Spectroscopy Logging System from the INEL. Both systems consist of essentially the same equipment, however, the INEL system is much more mobile and compact. The remainder of this section will focus on the INEL system. The test plan did not contain a detailed description of the INEL system because it was being constructed during preparation of the test plan. Therefore, a detailed description is included below.

The INEL Gamma Spectroscopy Logging System included a logging tool which was connected to various hardware and electronic equipment. The system was housed in a four-wheel drive Ford diesel van. Along with an AC generator, the van provided all power for the logging system. The system components are illustrated in Figure 2. The logging tool consisted of a 30% efficient, high-purity, germanium (HPGe) detector connected to a high voltage power supply and a pre-amplifier housed in a water-tight, stainless-steel casing. Both computer and manual controlled draw-works were used to raise and lower the logging tool once it was positioned inside a monitoring well. The liquid nitrogen (LN_2) cooling system was necessary for proper operation of the HPGe detector. The detector must be cryogenically cooled while being used in order to avoid damage to the crystal structure. An 800-foot long electrical cable connected the logging tool to the NIMBIN in the electronics cabinet. The output from the detector passed through the cable, and was processed in the NIMBIN multi-channel buffer (MCB). This cable also provided a vent tube for the LN_2 contained in the dewar. The data input cable rolled over a sheave wheel attached to a load pin and depth encoder. The load pin measured the total suspended load from the boom. The display of the load (in pounds) was located on the manual control panel. If the load increased above a default setting (caused by snagging the tool in a well case while coming out of a well), an alarm would sound and the system would halt. The depth encoder simply measured the length of cable that had rolled over the sheave wheel, and sent that information via a multi-conductor cable to the depth decoder. This data was then interpreted by the central processing unit and was displayed on both the manual control panel and on the display in the electronics cabinet.

Controls for positioning the logging tool were accessed either manually using the manual control panel or electronically using the keyboard in the electronics cabinet. In addition, the logging tool could be controlled by using a remote control located in the back of the van. This permitted easy and accurate positioning of the tool over a well. Essentially, all mechanical controls for the system could be accessed through the computer. Software developed specifically for the system allowed the user to control the entire system from the keyboard. Additionally, the user could control the method of data collection by providing the necessary information to the central processing unit. Data collection, or well monitoring could be performed in one of three modes: (1) acquire, (2) move-stop-acquire, and (3) continuous acquire. The first mode allowed the tool to be moved to a predetermined location. Once at the desired location, the system acquired a spectrum, or spectra, for a user-specified period of time. The second mode, move-stop-acquire, was more automated. The tool was positioned at a desired depth and through the use of the software, a stop location, the distance between samples, and the count time were entered into the system. The system then acquired the spectra at the specified depth intervals, and stored the files sequentially on the system hard drive. The third mode moved the logging tool, either up or down the well, at a constant velocity as specified

by the system operator. The operator also input the sample distance and the acquire time. For our purposes, counting times ranged from 80 to 600 seconds. The logging system then acquired and stored the data files sequentially. Output from the system was sent to either the display, disk, or a printer.

PROCEDURES

The activities performed during the infiltration test follow the guidance outlined in the Down-Hole Gamma Spectroscopic Monitoring System Test Plan (EGG-ER-11364, Rev 0), in addition to those outlined in the previous section on System Description. The design of a successful field experiment should closely follow the design laid out by Relyea (1982) for laboratory column experiments. The end result produced by following these design parameters is defensible and interpretable tracer breakthrough curves. All of the parameters discussed by Relyea (1982) are not measurable in the field (i.e., flow fracture length, fracture water velocity, etc.) but others, specifically boundary conditions, are prerequisite to obtaining BTCs. One such boundary condition is a known tracer input function (i.e., step or finite pulse input). The original experiment was designed for a step input of tracers. However, this was changed to a finite pulse input for two reasons: (1) the tracer supplier delivered only a fraction of the anticipated tracer quantities, and (2) mechanical problems were encountered with the tracer injection system which created radiological safety concerns. Therefore, in an effort to maximize the likelihood of observing BTCs, tracers were added as a finite pulse input six days after introduction of water to the basin. Breakthrough monitoring zones were to be selected during the first week (prior to tracer introduction) based on moisture data from the CPN and/or larger neutron probes. During this time, however, unsaturated zones were only detected in wells inside the basin. Additionally, only one basin well (A11A31) was accessible for monitoring by the gamma spectroscopy system, thus our efforts concentrated solely on well A11A31. This well served as the best chance of observing BTCs because of the pre-existing background data describing the subsurface geology.

Unfortunately, the occurrence of a violent thunder storm and subsequent safety precautions limited access to all basin area wells for three days after tracer introduction. This unusual occurrence effectively eliminated any chances of obtaining BTCs from well A11A31. Evidence supporting this is based on background data and data obtained after the storm showing that selenium and strontium reached maximum concentrations sometime during the three days following tracer introduction when access to the well was not allowed. Additionally, due to the conservative nature of selenium in basalt, transport theory predicts that the desorption side of the BTC would occur between zero and three days after introduction of clean water into the basin. Thus, our efforts shifted to monitoring two

basin wells, A11A31 by the INEL system and A01C11 by the Hanford system. Several tracer-containing intervals in each well were frequently monitored during the next two to three weeks, but no significant changes in selenium or strontium concentrations were observed. This indicates that subsurface flow patterns may have changed after tracer addition. In other words, tracer entered these zones but as hydrostatic pressure increased as the flow path filled with water or a dead-end fracture was filled, water flow shifted to other fractures. The net result of this situation would leave the water and associated tracers at the pre-observed locations, while additional water would follow another (adjacent) flowpath.

As mentioned earlier, a violent thunder storm occurred on July 31, 1994 and destroyed one of the piers, limited access to the remaining three (for 3 days). The storm blew some of the basin water over the containment berm, thus contaminating soil outside of the radiation control area. The presence of contaminated soil south and southeast of the basin resulted in closure of the road until survey crews confirmed the absence of soil contamination. Use of the gamma truck, significantly expedited identification of the one contaminated area and reopening of the road. This effort was completed by suspending the gamma tool from the back of the truck and taking measurements every 20 ft around the basin road. This procedure allowed a rapid and complete survey of the area since the counting radius of the detector in air is approximately 10 ft. Only one area was found to have counts significantly above background and this was roped off by a radiation control technician. A detour of the road around this area allowed the return of vehicle traffic around the basin.

Next, monitoring efforts were shifted to wells located outside of the basin, however, water only appeared in saturated zones located on the interbed. It was decided that constant monitoring of these zones was unwarranted because water samples could be obtained from these locations and analyzed by the mobile laboratory. Thus, efforts were shifted to profiling the tracer distribution in the wells in terms of counts per second versus depth.

Next, all pertinent spectral data were analyzed using Gamma Vision (EG&G Ortec) and Maestro II (EG&G Ortec). Analysis consisted of viewing each spectral file and identifying the tracer peaks. Each peak was marked and the analysis software was used to integrate the net peak area in terms of net counts per second. (Net peak area is equal to the total peak area minus the background.) This data was then compiled and plotted using Kaleidagraph data analysis and graphics software.

All data were backed up on 3.5 in. high-density diskettes. In addition, all logging activities were recorded in Environmental Restoration Program (ERP) Daily Activity Logbooks. Logbook entries consisted of well identification, file name, monitoring depth(s), logging sample duration, start

time, data, and operator identification. Field logbooks and original computer diskettes are on permanent file at the INEL ARDC.

RESULTS

One of the most significant contributions from the gamma spectroscopy monitoring systems was characterization of the field site with respect to tracer input and flow regimes in the subsurface. The change in input function should not have affected the outcome of the experiment, however, analysis of water sampling data indicated that use of the pulse input method was the primary reason usable tracer BTCs were obtained. In addition, lessons learned during the test indicated that the original design of a step input would have probably failed because of sorption/precipitation losses of tracers to the holding tank, transfer tubing, and tubing connections.

At the time of tracer input, the basin contained approximately 8.5 million gallons of water. The tracer input can be classified as a finite-pulse type if the basin was instantaneously mixed and no clean (non-tracer-containing) water was added to the basin until the original 8.5 million gallons had infiltrated. This approach was the one used, but evidence of complete and near-instantaneous mixing of the basin was required to prove that a finite-pulse input was achieved. Collection and analysis of water samples was planned to occur throughout basin mixing to determine when tracer concentrations inside the basin reached equilibrium. However, only one set of water samples was obtained prior to the violent storm and subsequent evacuation of the test site. Fortunately, during the tracer injection, the RLS (Hanford system) was monitoring the tracer concentration inside the basin. The detector was positioned 7.65 feet below the top of the casing in well A11A31. This placed the detector approximately at the midpoint of the water level in the basin. Results from these measurements are reported in counts per second (cps) in Table 1 and plotted in Figure 3. These data clearly show that the basin near the aquifer well was significantly mixed in approximately 150 minutes, which is a remarkably short time given the large volume of the basin. The success of the instantaneous mixing was primarily, and possibly solely, due to the use of three large mixing pumps which were operating during and after tracer addition. Without the near-instantaneous mixing, BTCs would have been less pronounced and right-hand skewed, and would probably not have been interpretable using current modeling approaches.

Another requirement suggested by Relyea (1982) for designing and implementing a successful tracer test concerns preferential flow patterns. Typically, preferential flow patterns are to be avoided in constructing columns, but since we are dealing with a fractured media, preferential flow is normal. The situation we had to avoid was modifying or increasing preferential flow patterns

during the installation of monitoring wells. Because we had numerous monitoring wells inside the basin, if water had flowed down the annular space of the wells, it could have been a significant source of water to the subsurface. The presence of water flow down the annular space of five basin wells was evaluated using the gamma tool.

The results from the gamma tool are presented in Tables 2-4 and Figures 4-6a for wells A01C11, A11C12, and A11A31, respectively. Each of the data summaries presented in tabular form were compiled from the spectrum analysis software and crosschecked with the original after entry into the computer spreadsheet. No tracer was detected below land surface in two wells, A08C13 and A11C13. Figure 4 contains three plots: (1) a plot of the Se-75 activity versus depth (note the break in the plot between 5 and 70 cps), (2) a plot of the Sr-85 activity versus depth, and (3) the well completion diagram. Terbium-160 was only detected at the surface where it was strongly adsorbed to basin sediments. The first point to note in Figure 4 is the presence of Se and Sr at the land surface. Both radionuclides are probably present due to infiltration into the soil and Sr is probably adsorbed to surficial sediments. In addition, the gamma logs indicated the presence of several small fractures at 11.9, 15.9, 20.9, and ~25 ft. This portion of the well was completed with bentonite, but the caliper log shows measurable fractures at ~36, 38, and 44 ft. Based on the gamma log, other smaller fractures are probably present. The next tracer (Se and Sr) activity shows up at 58 to 63 ft and corresponds well with the sand interval (54-60 ft) shown in the completion diagram. The next sand completion interval (72-82 ft) also shows the presence of Se and Sr (from 74-84 ft). Other measurements of Se are at 93, 96, 100, 106, and 120 ft. Each of these measurements correspond to sand completion intervals and fracture/rubble systems in the subsurface.

The next cross-section shown is that of well A11C12 (Figure 5). This figure is presented using the same format as that described previously for Figure 4. For this well, TB-160 was only detected at the land surface and was probably due solely to adsorption to the basin sediments. Selenium and strontium were also detected at the surface with an additional strong peak at ~20 ft. The caliper log does not show a fracture here, but the detection of both selenium and strontium strongly suggest that one is present (possibly a fracture just outside the radius of the borehole). The next detection of tracer (Se and Sr) occurs from 51 to 60 ft which corresponded to the sand interval shown in the completion diagram. Selenium and strontium activity were again strong at the 62-69 sand interval. Tracer was also found at the 82-87, 89-95, 101-111, and 114.5-127 zones. It is important to note that even the 2 ft bentonite seal between zones 82-87 and 89-95 ft appears to be effective in eliminating tracer movement between the two zones. Evidence for this is the lack of the strontium activity at 88 ft and the significant difference in selenium activity between the two sand-completed zones.

A similar plot was constructed for well A11A31 and is shown in Figure 6a. Measurable amounts of selenium and strontium activity were observed at the surface, possibly due to their presence in the basin water or due to surface infiltration or adsorption. As with the other basin wells, little to no activity was observed in the bentonite zones, but tracer was observed in the top four sand completion zones. Additionally, Figure 6b shows the infiltration of Tb-160 into the surficial sediment of the basin. Based on the data in Figure 6b, there is some evidence of a fracture at ~14 ft.

The next set of data deals with an unexpected observation. In an effort to compare results from the gamma truck to those obtained in the mobile laboratory, gamma probe measurements were taken in wells containing tracers (as determined by lab analysis). Results from these measurements are given in Tables 5-12 and Figures 7-14. Data are reported in counts per second as a function of depth from the top of the well casing. These results will be compared to laboratory measurements after the gamma probe is calibrated in Grand Junction. Data for this calibration was collected in November, 1994 and is currently being processed. Data conversion from cps to pCi/g or pCi/mL will be performed as necessary after the correction factors have been calculated. The point to note is that water samples collected using bailers represent an average water concentration, and significant differences in tracer concentration may occur at different, discrete depths. Figures 7-10 illustrate tracer concentrations that appear to be evenly distributed; as the probe was lowered into the water, the concentration reached a maximum value which remained the same to the bottom of the well. In contrast, several wells showed distinctly different profiles. These are shown in Figures 11-14. In some cases, the concentration consistently increased as the depth increased (Figures 12 and 14), while in others there appeared to be a spike of tracer at the bottom of the well (Figures 11 and 13). The differences between these two data sets are a direct result of in-situ vs. lab measurements. The lab measurement is based on a water sample collected over the entire bailer length of 3 ft, while the gamma probe can distinguish differences every 0.5 ft. The depth-discrete sensitivity of the gamma probe allows it to detect differences in media porosity (the higher the porosity, the higher the water content and the higher the mass of tracer measured) and subtle flow paths (water flow may be along the top, middle, or bottom of a zone). Either of these could account for the observed differences.

Similar depth-discrete results were evaluated for zones containing tracers in the basin wells. These transmissive zones can result from microfractures, rubble zones, or small sedimentary interbeds. Results from the gamma scans are shown in Figures 15-21 and are simply expansions of the depth scale of results given in Figures 4-6. Three zones from well A11C12, two from A01C11, and two from A11A31 are shown. Each of these zones contain a highly uneven distribution of tracers. This can most easily be explained by the proximity of individual measurements to

subsurface fractures around the monitoring well. Again, these results demonstrate the special high resolution of the gamma monitoring system.

CONCLUSIONS

Even though the initial objectives of the test were modified, there was a multitude of data and subsequent information derived from the use of the INEL Gamma Spectroscopy Logging System. The most obvious and pertinent application was the monitoring well completion and subsurface site characterization verification.

Two firm conclusions can be made based on the results of the monitoring well cross-sections. First, the well installation techniques used for the basin wells were highly effective in isolating different well (flow) zones. No leaks around the bentonite seal or connectivity between different sand zones was observed for any of the five wells tested. Second, installation of monitoring wells inside the basin did not increase the infiltration rate of the basin by allowing water to flow down the annular space of the boreholes. No tracer movement was observed through an entire zone of bentonite. Since these five wells represent the deepest wells installed in the basin (typically all down to the interbed), it is probably safe to assume that the remaining wells were installed with equal integrity. Additionally, the implications of the comparison between the water sampling data and the depth-discrete gamma spectroscopy data are as follows:

- The gamma probe may be more sensitive to tracer movement and concentration since it can sample (monitor) more discrete intervals, and

- Future investigations utilizing this probe could greatly increase our knowledge of tracer movement in the subsurface.

The conclusions of this component of the infiltration test are summarized below:

(1) Results show that the basin was completely mixed in approximately 150 minutes,

(2) Results show that the installation of wells did not increase the infiltration of water due to flow down the annular space of boreholes,

(3) Based on results 1 and 2, it can be concluded that a successful finite pulse injection of tracers was implemented, and

(4) Results suggest that water sampling may only represent an average tracer concentration and tracers within a fracture, rubble, or interbed zone may not be evenly distributed.

REFERENCES

Dunnivant, F. M., G. T. Norrell, G. D. Mecham, *Integrated Large-Scale Aquifer Pumping and Infiltration Tests: Down-Hole Gamma Spectroscopic Monitoring System Test Plan,* EGG-ER-11364, July 1994, Rev. 0.

Relyea, John F., 1982, "Theoretical and Experimental Considerations for the Use of the Column Method for Determining Retardation Factors," *Radioactive Waste Management and the Nuclear Fuel Cycle, Volume 3(2),* December 1982, pp. 151-166.

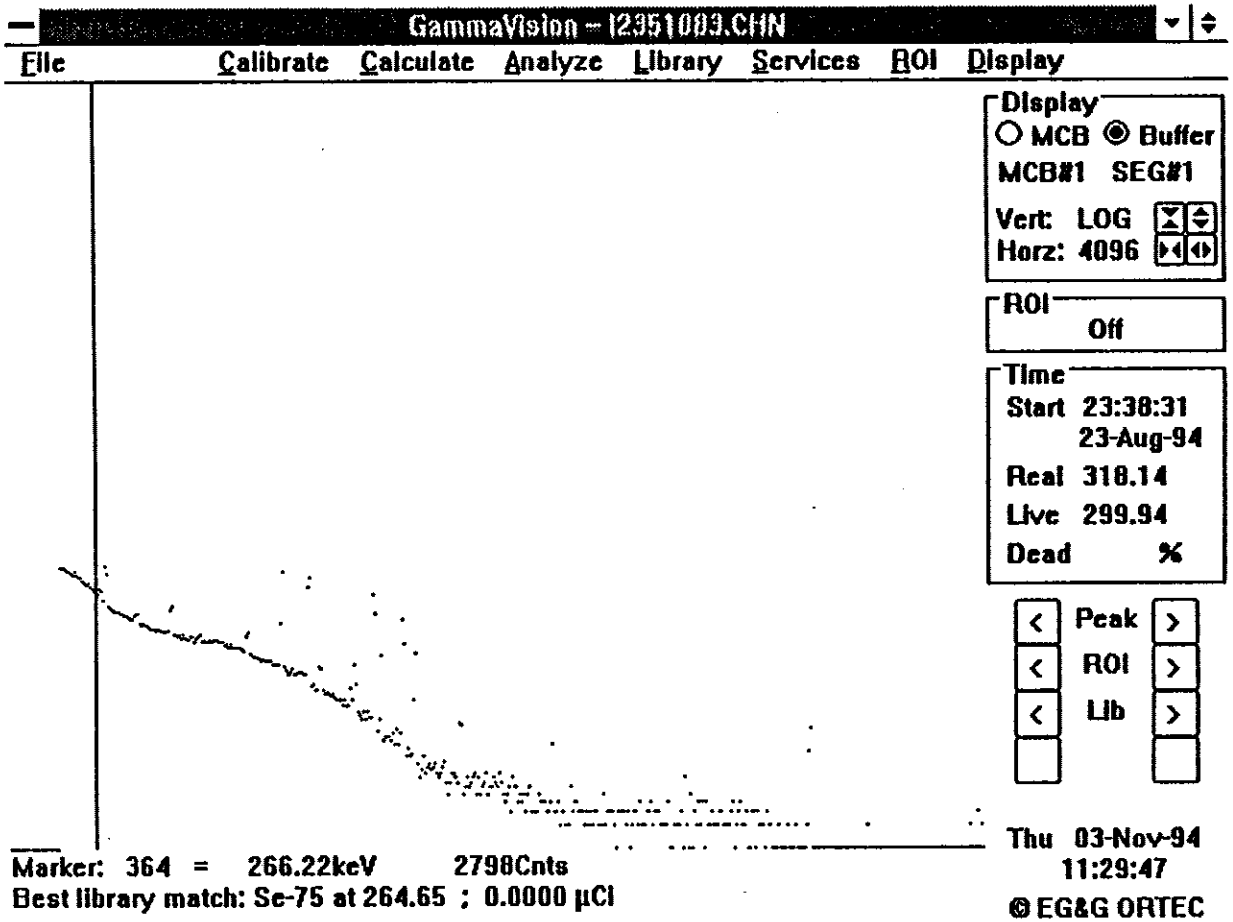

Figure 1. Typical gamma ray spectrum (software courtesy of EG&G Ortec).

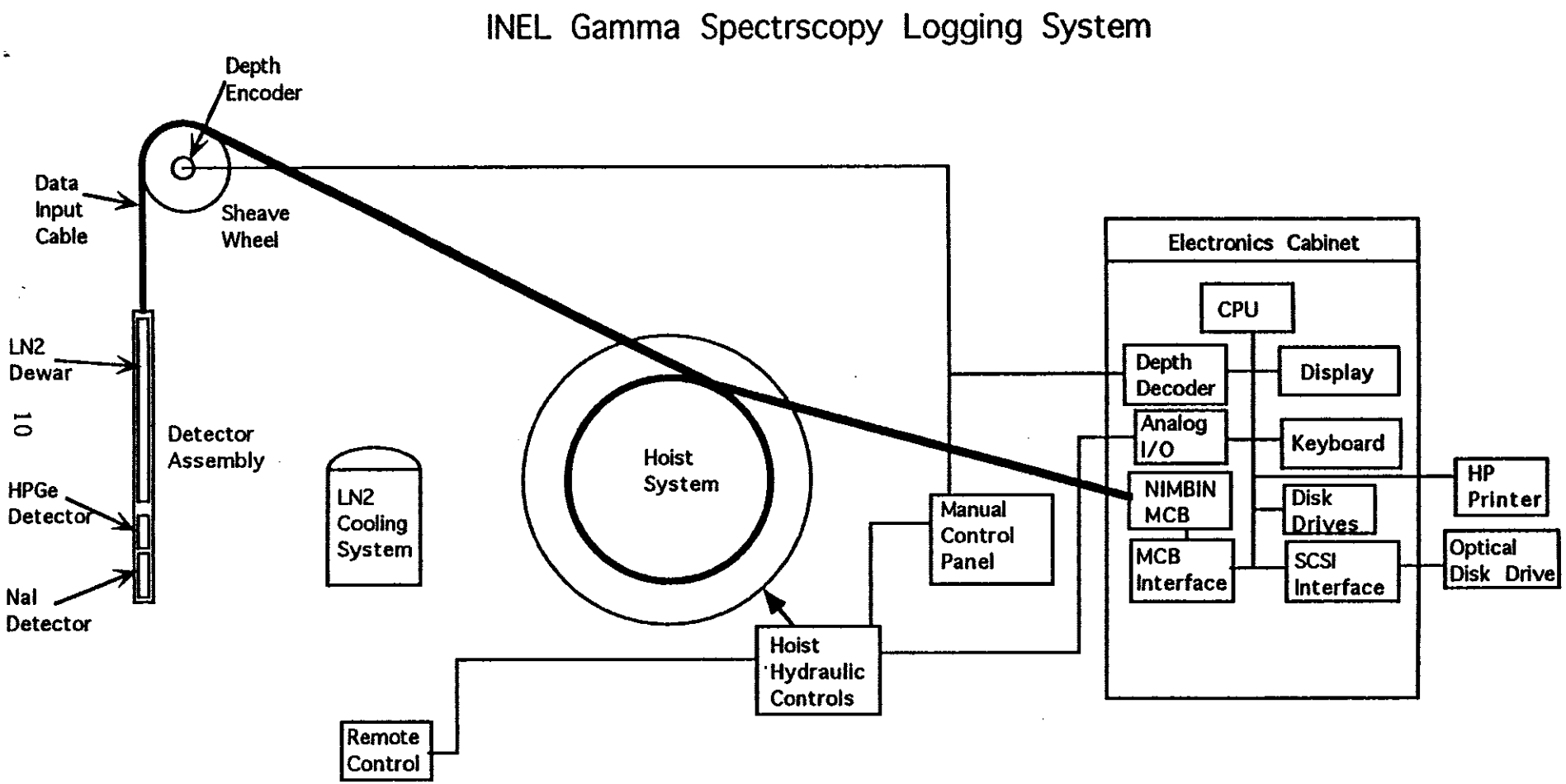

Figure 2. Schematic of the INEL Gamma Spectroscopy Monitoring System.

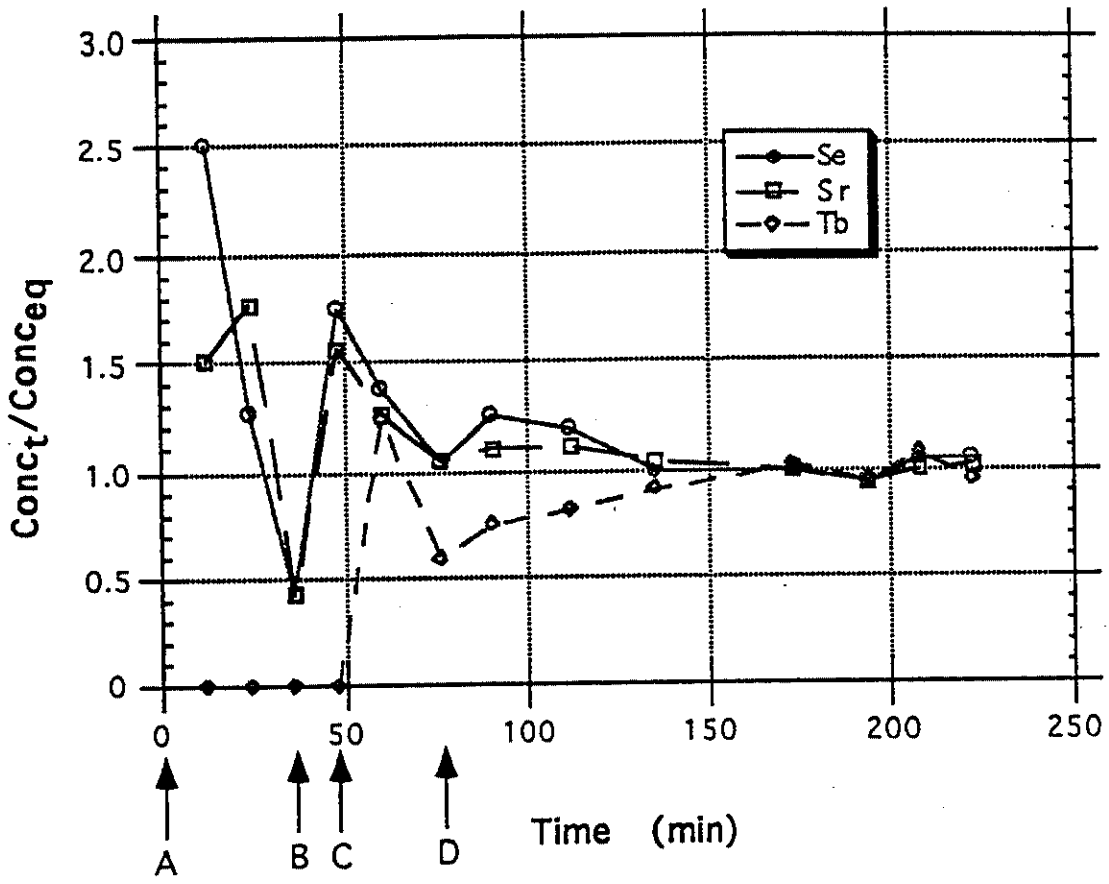

A Addition of Se and Sr solution to basin.
B Addition of Se and Sr tank wash water to basin.
C Addition of Tb solution to basin.
D Addition of acid wash of both tanks to basin.

Figure 3. Tracer concentrations in the infiltration basin as a function of time: basin approach to equilibrium.

Table 1. Results from gamma spectroscopy monitoring of basin during and after tracer input.

Time After Tracer Addition (min)	Se-75 cps[a]	Se-75 C_t/C_{Eq}[b]	Sr-85 cps	Sr-85 C_t/C_{Eq}[c]	Tb-160 cps	Tb-160 C_t/C_{Eq}[d]
	No Data	No Data	No Data	No Data	No Data	No Data
12	21.92	2.51	8.56	1.51	0	0
24	11.05	1.27	10.06	1.77	0	0
36	3.74	0.43	2.46	0.43	0	0
48	15.27	1.75	8.87	1.56	0	0
60	12.08	1.38	7.13	1.26	23.66	1.24
76	9.12	1.04	5.95	1.05	11.31	0.59
90	11.04	1.26	6.22	1.10	14.34	0.75
112	10.40	1.19	6.27	1.11	15.70	0.82
135	8.60	0.99	5.90	1.04	17.30	0.91
173	8.61	0.99	5.66	1.00	19.45	1.02
194	8.23	0.94	5.35	0.94	18.20	0.95
208	9.05	1.04	5.65	1.00	20.50	1.07
222	9.15	1.05	5.8	1.02	18.20	0.95

a cps is counts per second

b C_t/C_{Eq} is the concentration at a given time divided by the equilibrium concentration of the basin. The equilibrium concentration of the basin is the average of the last 5 numbers in the Se-75 cps column (average = 8.73 cps).

c The equilibrium concentration of the basin is the average of the last 5 numbers in the Sr-85 cps column (average = 5.67 cps).

d The equilibrium concentration of the basin is the average of the last 4 numbers in the Tb-160 cps column (average = 10.09 cps).

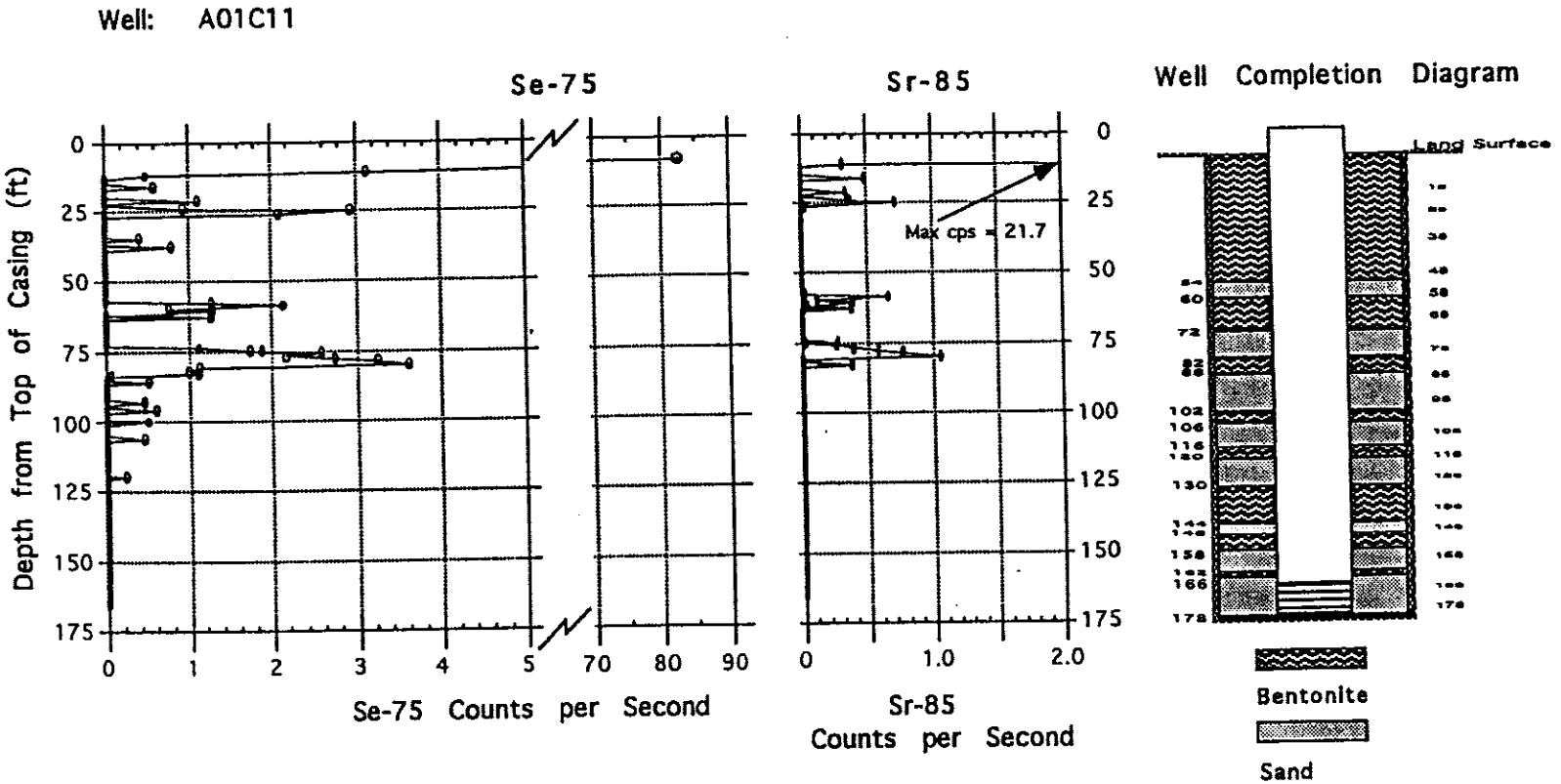

Figure 4. Gamma spectroscopy cross section of Se-75, Sr-85, and completion diagram for Well A01C11 (AB).

Table 2. Gamma spectroscopy cross section data for Well A01C11 (AB) (data collected on August 31, 1994).

	Depth (ft)	Se-75 cps	Sr-85 cps	Tb-160 cps	E
1	7.9000	82.690	21.680	52.560	
2	8.9000	24.150	14.390	0.37000	
3	9.9000	7.9900	8.6600	0.0000	
4	10.900	3.1300	0.32000	0.18000	
5	11.900	0.50000	0.0000	0.0000	
6	12.900	0.0000	0.0000	0.0000	
7	13.900	0.0000	0.0000	0.0000	
8	14.900	0.0000	0.0000	0.0000	
9	15.900	0.59000	0.49000	0.0000	
10	16.900	0.0000	0.0000	0.0000	
11	17.900	0.0000	0.0000	0.0000	
12	18.900	0.0000	0.0000	0.0000	
13	19.900	0.0000	0.0000	0.0000	
14	20.900	1.1200	0.34000	0.0000	
15	21.900	0.0000	0.0000	0.0000	
16	22.900	0.0000	0.0000	0.0000	
17	23.900	0.95000	0.38000	0.0000	
18	24.900	2.9400	0.72000	0.60000	
19	25.900	2.1000	0.030000	0.0000	
20	26.900	0.0000	0.0000	0.0000	
21	27.900	0.0000	0.0000	0.0000	
22	28.900	0.0000	0.0000	0.0000	
23	29.900	0.0000	0.0000	0.0000	
24	30.900	0.0000	0.0000	0.0000	
25	31.900	0.0000	0.0000	0.0000	
26	32.900	0.0000	0.0000	0.0000	
27	33.900	0.0000	0.0000	0.0000	
28	34.900	0.42000	0.0000	0.0000	
29	35.900	0.0000	0.0000	0.0000	
30	36.900	0.0000	0.0000	0.0000	
31	37.900	0.82000	0.0000	0.0000	
32	38.900	0.0000	0.0000	0.0000	
33	39.900	0.0000	0.0000	0.0000	
34	40.900	0.0000	0.0000	0.0000	
35	41.900	0.0000	0.0000	0.0000	
36	42.900	0.0000	0.0000	0.0000	
37	43.900	0.0000	0.0000	0.0000	
38	44.900	0.0000	0.0000	0.0000	
39	45.900	0.0000	0.0000	0.0000	
40	46.900	0.0000	0.0000	0.0000	
41	47.900	0.0000	0.0000	0.0000	
42	48.900	0.0000	0.0000	0.0000	
43	49.900	0.0000	0.0000	0.0000	
44	50.900	0.0000	0.0000	0.0000	
45	51.900	0.0000	0.0000	0.0000	
46	52.900	0.0000	0.0000	0.0000	
47	53.900	0.0000	0.0000	0.0000	

Table 2. (continued).

	Depth (ft)	Se-75 cps	Sr-85 cps	Tb-160 cps	E
48	54.900	0.0000	0.0000	0.0000	
49	55.900	0.0000	0.0000	0.0000	
50	56.900	0.0000	0.0000	0.0000	
51	57.900	1.2900	0.020000	0.0000	
52	58.900	2.1500	0.66000	0.0000	
53	59.900	0.77000	0.12000	0.0000	
54	60.900	1.3000	0.39000	0.0000	
55	61.900	0.0000	0.040000	0.0000	
56	62.900	1.2800	0.38000	0.0000	
57	63.900	0.0000	0.0000	0.0000	
58	64.900	0.0000	0.0000	0.0000	
59	65.900	0.0000	0.0000	0.0000	
60	66.900	0.0000	0.0000	0.0000	
61	67.900	0.0000	0.0000	0.0000	
62	68.900	0.0000	0.0000	0.0000	
63	69.900	0.0000	0.0000	0.0000	
64	70.900	0.0000	0.0000	0.0000	
65	71.900	0.0000	0.0000	0.0000	
66	72.900	0.0000	0.0000	0.0000	
67	73.900	1.1300	0.0000	0.0000	
68	74.900	1.8900	0.27000	0.0000	
69	75.000	1.7500	0.020000	0.0000	
70	76.000	2.5800	0.26000	0.0000	
71	77.000	2.1800	0.39000	0.0000	
72	78.000	2.7400	0.58000	0.0000	
73	79.000	3.2500	0.77000	0.0000	
74	80.000	3.6200	1.0600	0.0000	
75	81.000	1.1400	0.0000	0.0000	
76	82.000	1.0000	0.0000	0.0000	
77	83.000	1.1200	0.38000	0.0000	
78	84.000	0.060000	0.0000	0.0000	
79	85.000	0.0000	0.0000	0.0000	
80	86.000	0.52000	0.0000	0.0000	
81	87.000	0.0000	0.0000	0.0000	
82	88.000	0.0000	0.0000	0.0000	
83	89.000	0.0000	0.0000	0.0000	
84	90.000	0.0000	0.0000	0.0000	
85	91.000	0.0000	0.0000	0.0000	
86	92.000	0.0000	0.0000	0.0000	
87	93.000	0.47000	0.0000	0.0000	
88	94.000	0.0000	0.0000	0.0000	
89	95.000	0.0000	0.0000	0.0000	
90	96.000	0.61000	0.0000	0.0000	
91	97.000	0.0000	0.0000	0.0000	
92	98.000	0.0000	0.0000	0.0000	
93	99.000	0.0000	0.0000	0.0000	
94	100.00	0.51000	0.0000	0.0000	

Table 2. (continued).

	Depth (ft)	Se-75 cps	Sr-85 cps	Tb-160 cps	E
95	101.00	0.0000	0.0000	0.0000	
96	102.00	0.0000	0.0000	0.0000	
97	103.00	0.0000	0.0000	0.0000	
98	104.00	0.0000	0.0000	0.0000	
99	105.00	0.0000	0.0000	0.0000	
100	106.00	0.46000	0.0000	0.0000	
101	107.00	0.0000	0.0000	0.0000	
102	108.00	0.0000	0.0000	0.0000	
103	109.00	0.0000	0.0000	0.0000	
104	110.00	0.0000	0.0000	0.0000	
105	111.00	0.0000	0.0000	0.0000	
106	112.00	0.0000	0.0000	0.0000	
107	113.00	0.0000	0.0000	0.0000	
108	114.00	0.0000	0.0000	0.0000	
109	115.00	0.0000	0.0000	0.0000	
110	116.00	0.0000	0.0000	0.0000	
111	117.00	0.0000	0.0000	0.0000	
112	118.00	0.0000	0.0000	0.0000	
113	119.00	0.0000	0.0000	0.0000	
114	120.00	0.22000	0.0000	0.0000	
115	121.00	0.0000	0.0000	0.0000	
116	122.00	0.0000	0.0000	0.0000	
117	123.00	0.0000	0.0000	0.0000	
118	124.00	0.0000	0.0000	0.0000	
119	125.00	0.0000	0.0000	0.0000	
120	126.00	0.0000	0.0000	0.0000	
121	127.00	0.0000	0.0000	0.0000	
122	128.00	0.0000	0.0000	0.0000	
123	129.00	0.0000	0.0000	0.0000	
124	130.00	0.0000	0.0000	0.0000	
125	131.00	0.0000	0.0000	0.0000	
126	132.00	0.0000	0.0000	0.0000	
127	133.00	0.0000	0.0000	0.0000	
128	134.00	0.0000	0.0000	0.0000	
129	135.00	0.0000	0.0000	0.0000	
130	136.00	0.0000	0.0000	0.0000	
131	137.00	0.0000	0.0000	0.0000	
132	138.00	0.0000	0.0000	0.0000	
133	139.00	0.0000	0.0000	0.0000	
134	140.00	0.0000	0.0000	0.0000	
135	141.00	0.0000	0.0000	0.0000	
136	142.00	0.0000	0.0000	0.0000	
137	143.00	0.0000	0.0000	0.0000	
138	144.00	0.0000	0.0000	0.0000	
139	145.00	0.0000	0.0000	0.0000	
140	146.00	0.0000	0.0000	0.0000	
141	147.00	0.0000	0.0000	0.0000	

Table 2. (continued).

	Depth (ft)	Se-75 cps	Sr-85 cps	Tb-160 cps	E
142	148.00	0.0000	0.0000	0.0000	
143	149.00	0.0000	0.0000	0.0000	
144	150.00	0.0000	0.0000	0.0000	
145	151.00	0.0000	0.0000	0.0000	
146	152.00	0.0000	0.0000	0.0000	
147	153.00	0.0000	0.0000	0.0000	
148	154.00	0.0000	0.0000	0.0000	
149	155.00	0.0000	0.0000	0.0000	
150	156.00	0.0000	0.0000	0.0000	
151	157.00	0.0000	0.0000	0.0000	
152	158.00	0.0000	0.0000	0.0000	
153	159.00	0.0000	0.0000	0.0000	
154	160.00	0.0000	0.0000	0.0000	
155	161.00	0.0000	0.0000	0.0000	
156	162.00	0.0000	0.0000	0.0000	
157	163.00	0.0000	0.0000	0.0000	
158	164.00	0.0000	0.0000	0.0000	
159	165.00	0.0000	0.0000	0.0000	

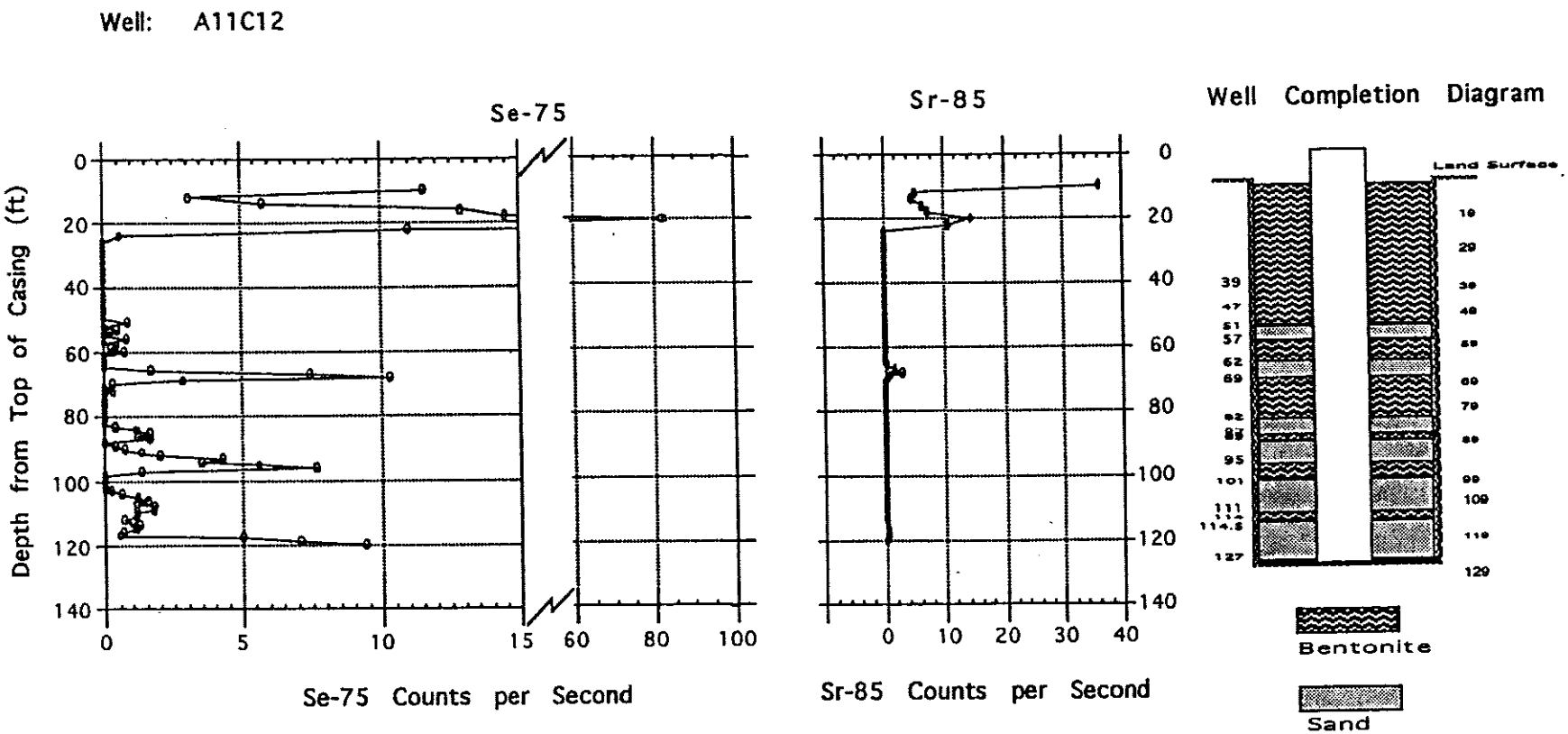

Figure 5. Gamma spectroscopy cross section of Se-75, Sr-85, and completion diagram for Well A11C12 (MD).

Table 3. Gamma spectroscopy cross section data for Well A11C12 (MD) (data collected on August 29, 1994).

	Depth	Se-75	Sr-85
1	10.000	11.600	36.200
2	12.000	3.1000	5.2900
3	14.000	5.8400	4.7600
4	16.000	12.900	6.4300
5	18.000	14.500	7.3200
6	20.000	82.200	14.500
7	22.000	11.000	10.700
8	24.000	0.57000	0.0000
9	26.000	0.0000	0.0000
10	28.000	0.0000	0.0000
11	29.000	0.0000	0.0000
12	30.000	0.0000	0.0000
13	32.000	0.0000	0.0000
14	34.000	0.0000	0.0000
15	36.000	0.0000	0.0000
16	38.000	0.0000	0.0000
17	40.000	0.0000	0.0000
18	42.000	0.0000	0.0000
19	44.000	0.0000	0.0000
20	46.000	0.0000	0.0000
21	48.000	0.0000	0.0000
22	50.000	0.0000	0.0000
23	51.000	0.86000	0.0000
24	52.000	0.0000	0.0000
25	53.000	0.45000	0.0000
26	54.000	0.23000	0.0000
27	55.000	0.0000	0.0000
28	56.000	0.82000	0.0000
29	57.000	0.0000	0.0000
30	58.000	0.41000	0.0000
31	59.000	0.22000	0.0000
32	60.000	0.72000	0.0000
33	61.000	0.0000	0.0000
34	62.000	0.0000	0.0000
35	63.000	0.0000	0.0000
36	64.000	0.0000	0.0000
37	65.000	0.0000	0.0000
38	66.000	1.7000	0.40000
39	67.000	7.4400	1.7300
40	68.000	10.300	2.9300
41	69.000	2.8300	0.98000
42	70.000	0.29000	0.42000
43	71.000	0.0000	0.0000
44	72.000	0.31000	0.0000
45	73.000	0.0000	0.0000
46	74.000	0.0000	0.0000
47	75.000	0.0000	0.0000
48	76.000	0.0000	0.0000
49	77.000	0.0000	0.0000
50	78.000	0.0000	0.0000
51	79.000	0.0000	0.0000
52	80.000	0.0000	0.0000
53	81.000	0.0000	0.0000
54	82.000	0.0000	0.0000
55	83.000	0.36000	0.0000
56	84.000	1.1600	0.0000
57	85.000	1.6300	0.0000
58	86.000	1.2300	0.0000
59	87.000	1.6500	0.21000
60	88.000	0.0000	0.0000
61	89.000	0.37000	0.0000
62	90.000	0.73000	0.0000
63	91.000	1.3400	0.0000
64	92.000	2.0100	0.0000
65	93.000	4.2800	0.0000
66	94.000	3.4900	0.0000
67	95.000	5.6300	0.0000
68	96.000	7.6500	0.0000
69	97.000	1.3300	0.0000
70	98.000	0.0000	0.0000
71	99.000	0.0000	0.0000
72	100.00	0.0000	0.0000
73	101.00	0.0000	0.0000
74	102.00	0.0000	0.0000
75	103.00	0.23000	0.0000
76	104.00	0.58000	0.0000
77	105.00	1.1800	0.25000
78	106.00	1.5500	0.0000
79	107.00	1.1700	0.0000
80	108.00	1.7800	0.0000
81	109.00	1.7600	0.0000
82	110.00	1.1500	0.0000
83	111.00	1.1400	0.0000
84	112.00	0.70000	0.0000
85	113.00	1.0000	0.0000
86	114.00	1.2500	0.0000
87	115.00	1.1200	0.25000
88	116.00	0.65000	0.26000
89	117.00	0.53000	0.43000
90	118.00	5.0000	0.31000
91	119.00	7.0900	0.45000
92	120.00	9.4000	0.0000

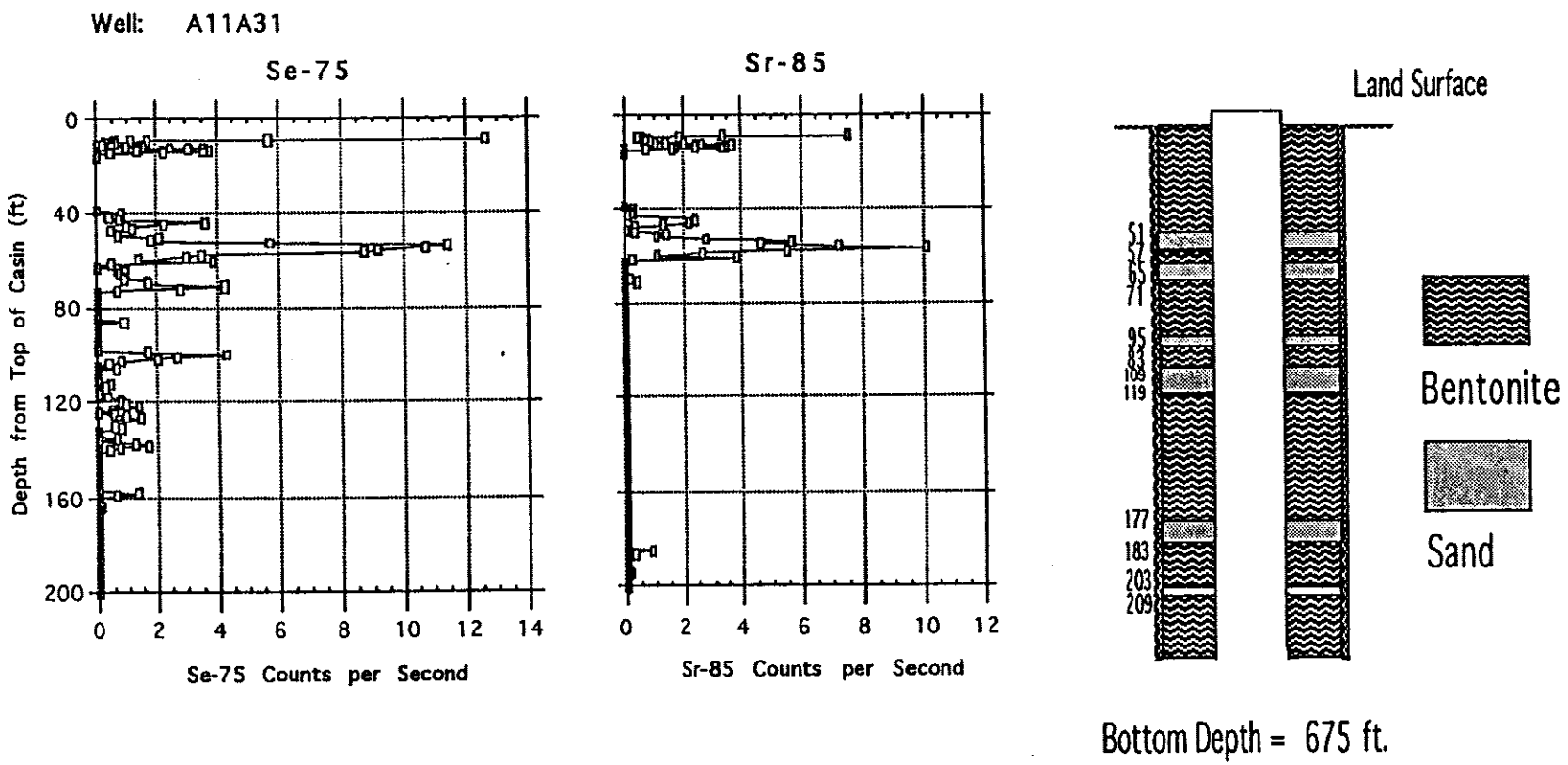

Figure 6a. Gamma spectroscopy cross section of Se-75, Sr-85, and completion diagram for Well A11A31 (MA).

Table 4. Gamma spectroscopy cross section data for Well A11A31 (MA) (data collected on August 17, 1994).

	Depth	Se-75 cps	Sr-85 cps	Tb-160
1	9.0000	12.650	7.5300	34.340
2	9.2500	5.6600	3.3500	18.550
3	9.5000	1.7100	1.8800	6.0500
4	9.7500	1.1400	0.58000	2.0900
5	10.000	0.60000	0.43000	0.62000
6	10.250	0.29000	0.72000	0.29000
7	10.500	0.61000	0.77000	0.14000
8	10.750	0.43000	0.77000	0.0000
9	11.000	0.22000	0.64000	0.12000
10	11.250	0.0000	0.70000	0.24000
11	11.500	0.52000	0.89000	0.30000
12	11.750	0.49000	1.0700	0.56000
13	12.000	1.0100	1.4100	0.69000
14	12.250	1.5500	2.0000	0.73000
15	12.500	2.4900	2.6600	0.79000
16	12.750	3.5900	3.7100	0.58000
17	13.000	3.1000	3.2600	0.46000
18	13.250	1.4300	2.4700	0.49000
19	13.500	1.3600	1.7100	0.83000
20	13.750	2.2600	2.4200	1.4700
21	14.000	3.7600	3.4900	2.0000
22	14.250	3.5900	3.3400	2.5100
23	14.500	2.2500	1.6100	1.5000
24	14.750	0.45667	0.71000	0.68000
25	15.000	0.0000	0.0000	0.36000
26	15.250	0.0000	0.0000	0.090000
27	15.500	0.0000	0.0000	0.0000
28	15.750	0.0000	0.0000	0.0000
29	16.000	0.0000	0.0000	0.0000
30	39.000	0.0000	0.0000	0.0000
31	40.000	0.83333	0.28333	0.0000
32	41.000	0.33333	0.083333	0.0000
33	42.000	0.42222	0.23889	0.0000
34	43.000	0.73333	0.11667	0.0000
35	44.000	3.6222	2.4056	0.0000
36	45.000	2.2556	2.4333	0.0000
37	46.000	1.0056	2.1778	0.0000
38	47.000	1.2167	1.2944	0.0000
39	48.000	0.45556	0.31667	0.0000
40	49.000	0.71111	0.072222	0.0000
41	50.000	0.71111	0.30556	0.0000
42	51.000	2.1167	1.4278	0.0000
43	52.000	1.7889	1.0778	0.0000
44	53.000	5.7167	2.7889	0.0000
45	54.000	11.417	5.6722	0.0000
46	55.000	10.711	4.6167	0.0000
47	56.000	9.1722	7.2111	0.0000

Table 4. (continued).

	Depth	Se-75 cps	Sr-85 cps	Tb-160
48	57.000	8.7278	10.089	0.0000
49	58.000	3.5056	5.5389	0.0000
50	59.000	2.9833	2.6889	0.0000
51	60.000	1.4000	1.1000	0.0000
52	61.000	3.8611	3.8278	0.0000
53	62.000	0.45000	0.26667	0.0000
54	63.000	0.0000	0.0055556	0.0000
55	64.000	0.66111	0.0000	0.0000
56	65.000	0.95556	0.0000	0.0000
57	66.000	0.73889	0.0000	0.0000
58	67.000	0.90000	0.0000	0.0000
59	68.000	0.92222	0.0000	0.0000
60	69.000	1.6944	0.055556	0.0000
61	70.000	1.7389	0.17778	0.0000
62	71.000	4.2375	0.40000	0.0000
63	72.000	2.7875	0.0000	0.0000
64	73.000	0.65000	0.0000	0.0000
65	74.000	0.0000	0.0000	0.0000
66	75.000	0.0000	0.0000	0.0000
67	76.000	0.0000	0.0000	0.0000
68	77.000	0.0000	0.0000	0.0000
69	78.000	0.0000	0.0000	0.0000
70	79.000	0.0000	0.0000	0.0000
71	80.000	0.0000	0.0000	0.0000
72	81.000	0.0000	0.0000	0.0000
73	82.000	0.0000	0.0000	0.0000
74	83.000	0.0000	0.0000	0.0000
75	84.000	0.0000	0.0000	0.0000
76	85.000	0.0000	0.0000	0.0000
77	86.000	0.88750	0.0000	0.0000
78	87.000	0.0000	0.0000	0.0000
79	88.000	0.0000	0.0000	0.0000
80	89.000	0.0000	0.0000	0.0000
81	90.000	0.0000	0.0000	0.0000
82	91.000	0.0000	0.0000	0.0000
83	92.000	0.0000	0.0000	0.0000
84	93.000	0.0000	0.0000	0.0000
85	94.000	0.0000	0.0000	0.0000
86	95.000	0.0000	0.0000	0.0000
87	96.000	0.0000	0.0000	0.0000
88	97.000	0.0000	0.0000	0.0000
89	98.000	0.0000	0.0000	0.0000
90	99.000	1.6750	0.0000	0.0000
91	100.00	4.2750	0.0000	0.0000
92	101.00	2.6875	0.0000	0.0000
93	102.00	2.0125	0.0000	0.0000
94	103.00	0.77500	0.0000	0.0000

Table 4. (continued).

	Depth	Se-75 cps	Sr-85 cps	Tb-160
95	104.00	0.38750	0.0000	0.0000
96	105.00	0.0000	0.0000	0.0000
97	106.00	0.63750	0.0000	0.0000
98	107.00	0.0000	0.0000	0.0000
99	108.00	0.0000	0.0000	0.0000
100	109.00	0.0000	0.025000	0.0000
101	110.00	0.0000	0.0000	0.0000
102	111.00	0.0000	0.0000	0.0000
103	112.00	0.0000	0.0000	0.0000
104	113.00	0.42500	0.0000	0.0000
105	114.00	0.25000	0.0000	0.0000
106	115.00	0.0000	0.0000	0.0000
107	116.00	0.0000	0.0000	0.0000
108	117.00	0.0000	0.0000	0.0000
109	118.00	0.33750	0.0000	0.0000
110	119.00	0.73750	0.0000	0.0000
111	120.00	0.77500	0.0000	0.0000
112	121.00	0.93750	0.0000	0.0000
113	122.00	1.3875	0.0000	0.0000
114	123.00	0.46250	0.0000	0.0000
115	124.00	0.0000	0.0000	0.0000
116	125.00	0.55000	0.0000	0.0000
117	126.00	0.95000	0.0000	0.0000
118	127.00	1.4625	0.0000	0.0000
119	128.00	0.67500	0.0000	0.0000
120	129.00	0.73750	0.0000	0.0000
121	130.00	0.55000	0.0000	0.0000
122	131.00	0.77500	0.0000	0.0000
123	132.00	0.0000	0.0000	0.0000
124	133.00	0.0000	0.0000	0.0000
125	134.00	0.0000	0.0000	0.0000
126	135.00	0.61250	0.0000	0.0000
127	136.00	0.0000	0.0000	0.0000
128	137.00	1.2250	0.0000	0.0000
129	138.00	1.6750	0.0000	0.0000
130	139.00	0.72500	0.0000	0.0000
131	140.00	0.36250	0.0000	0.0000
132	141.00	0.0000	0.0000	0.0000
133	142.00	0.0000	0.0000	0.0000
134	143.00	0.0000	0.0000	0.0000
135	144.00	0.0000	0.0000	0.0000
136	145.00	0.0000	0.0000	0.0000
137	146.00	0.0000	0.0000	0.0000
138	147.00	0.0000	0.0000	0.0000
139	148.00	0.0000	0.0000	0.0000
140	149.00	0.0000	0.0000	0.0000
141	150.00	0.0000	0.0000	0.0000

Table 4. (continued).

	Depth	Se-75 cps	Sr-85 cps	Tb-160
142	151.00	0.0000	0.0000	0.0000
143	152.00	0.0000	0.0000	0.0000
144	153.00	0.0000	0.0000	0.0000
145	154.00	0.0000	0.0000	0.0000
146	155.00	0.0000	0.0000	0.0000
147	156.00	0.0000	0.0000	0.0000
148	157.00	0.0000	0.0000	0.0000
149	158.00	1.3250	0.0000	0.0000
150	159.00	0.57500	0.0000	0.0000
151	160.00	0.0000	0.0000	0.0000
152	161.00	0.0000	0.0000	0.0000
153	162.00	0.0000	0.0000	0.0000
154	163.00	0.0000	0.0000	0.0000
155	164.00	0.075000	0.0000	0.0000
156	165.00	0.0000	0.0000	0.0000
157	166.00	0.0000	0.0000	0.0000
158	167.00	0.0000	0.0000	0.0000
159	168.00	0.0000	0.0000	0.0000
160	169.00	0.0000	0.0000	0.0000
161	170.00	0.0000	0.0000	0.0000
162	171.00	0.0000	0.0000	0.0000
163	172.00	0.0000	0.0000	0.0000
164	173.00	0.0000	0.0000	0.0000
165	174.00	0.0000	0.0000	0.0000
166	175.00	0.0000	0.0000	0.0000
167	176.00	0.0000	0.0000	0.0000
168	177.00	0.0000	0.0000	0.0000
169	178.00	0.0000	0.0000	0.0000
170	179.00	0.0000	0.0000	0.0000
171	180.00	0.0000	0.0000	0.0000
172	181.00	0.0000	0.0000	0.0000
173	182.00	0.0000	0.0000	0.0000
174	183.00	0.0000	0.0000	0.0000
175	184.00	0.0000	0.0000	0.0000
176	185.00	0.0000	0.84615	0.0000
177	186.00	0.0000	0.0000	0.0000
178	187.00	0.0000	0.26250	0.0000
179	188.00	0.0000	0.0000	0.0000
180	189.00	0.0000	0.0000	0.0000
181	190.00	0.0000	0.0000	0.0000
182	191.00	0.0000	0.0000	0.0000
183	192.00	0.0000	0.0000	0.0000
184	193.00	0.0000	0.0000	0.0000
185	194.00	0.0000	0.11250	0.0000
186	195.00	0.0000	0.0000	0.0000
187	196.00	0.0000	0.0000	0.0000
188	197.00	0.0000	0.025000	0.0000

Table 4. (continued).

	Depth	Se-75 cps	Sr-85 cps	Tb-160
189	198.00	0.0000	0.0000	0.0000
190	199.00	0.0000	0.025000	0.0000
191	200.00	0.0000	0.0000	0.0000
192	201.00	0.0000	0.0000	0.0000
193	202.00	0.0000	0.40000	0.0000
194	203.00	0.0000	0.0000	0.0000
195	204.00	0.0000	0.0000	0.0000
196	205.00	0.0000	0.0000	0.0000
197	206.00	0.0000	0.0000	0.0000
198	207.00	0.0000	0.0000	0.0000
199	208.00	0.0000	0.0000	0.0000
200	209.00	0.0000	0.0000	0.0000

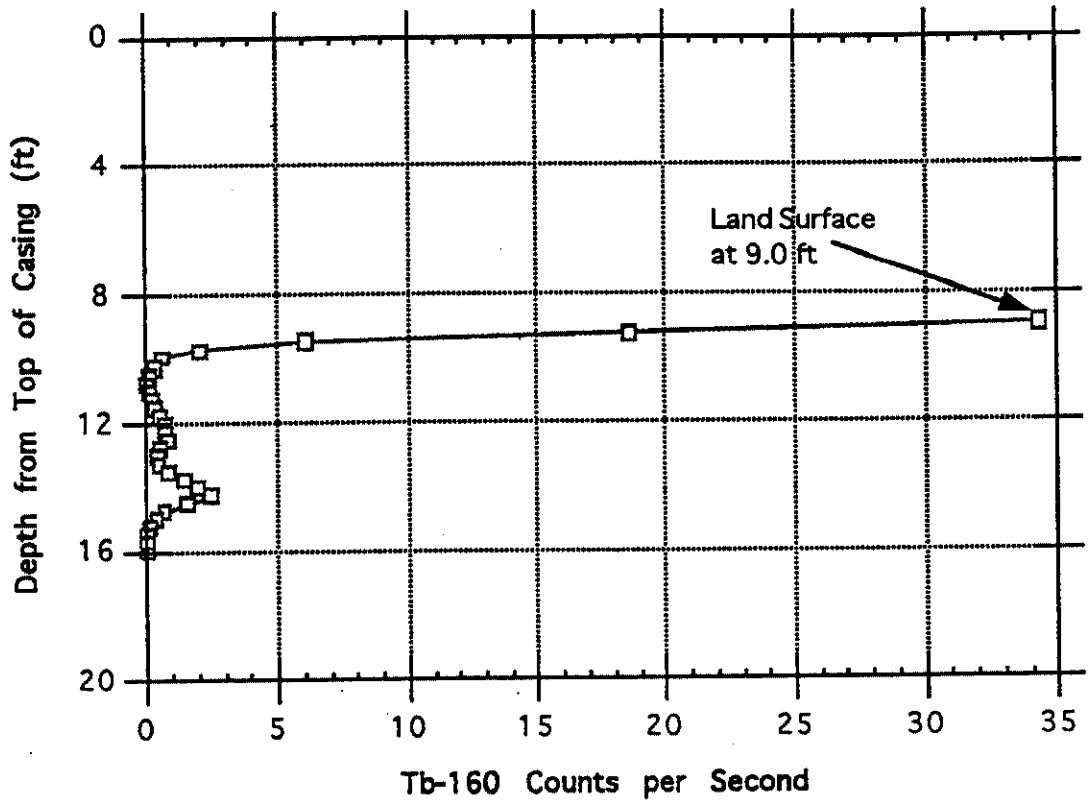

Figure 6b. Gamma spectroscopy cross section of TB-160 for the 9-16 ft zone of Well A11A31 (MA).

Table 5. Gamma spectroscopy cross section data for Well B05011 (FA) (data collected on August 27, 1994).

	Depth (ft)	Se-75 cps	C
1	173.00	0.0000	
2	173.50	0.0000	
3	174.00	0.040000	
4	174.50	0.15000	
5	175.00	0.82000	
6	175.50	0.98000	
7	176.00	1.0400	
8	176.50	1.2100	
9	177.00	1.3400	
10	177.50	1.2300	
11	178.00	1.1900	
12	178.50	1.2200	

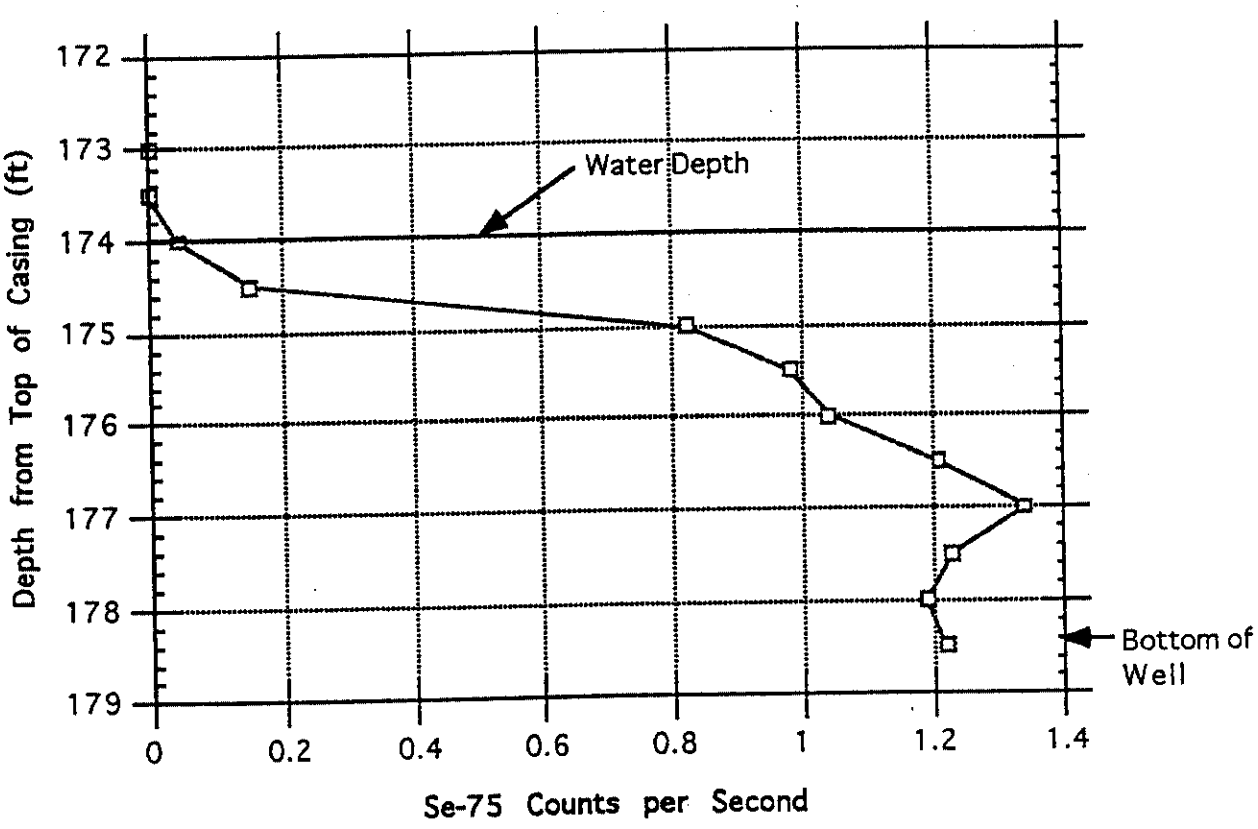

Figure 7. Selenium-75 counts per second vs. depth for the saturated zone of Well B05011 (FA).

Table 6. Gamma spectroscopy cross section data for Well B13N11 (OA) (data collected on August 30, 1994).

	Depth (ft)	Se-75 cps	C
1	174.00	0.0000	
2	175.00	0.0000	
3	176.00	0.0000	
4	177.00	0.32000	
5	178.00	0.91000	
6	179.00	0.90000	

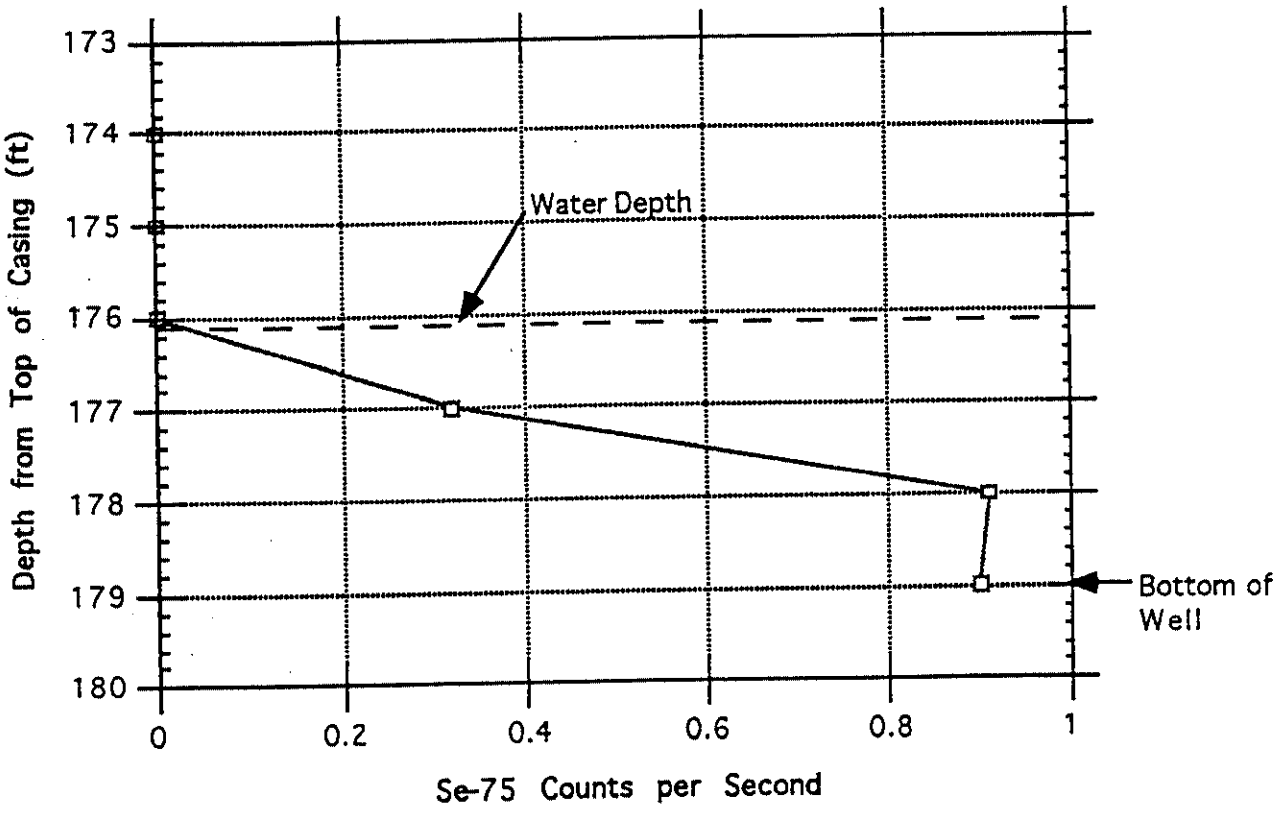

Figure 8. Selenium-75 counts per second vs. depth for the saturated zone of Well B13N11 (OA).

Table 7. Gamma spectroscopy cross section data for Well B12011 (NA) (data collected on August 30, 1994).

	Depth (ft)	Se-75 cps	C
1	174.00	0.0000	
2	175.00	0.0000	
3	176.00	0.0000	
4	177.00	0.46000	
5	178.00	0.38000	
6	179.00	0.51000	
7	180.00	0.38000	
8	181.00	0.59000	

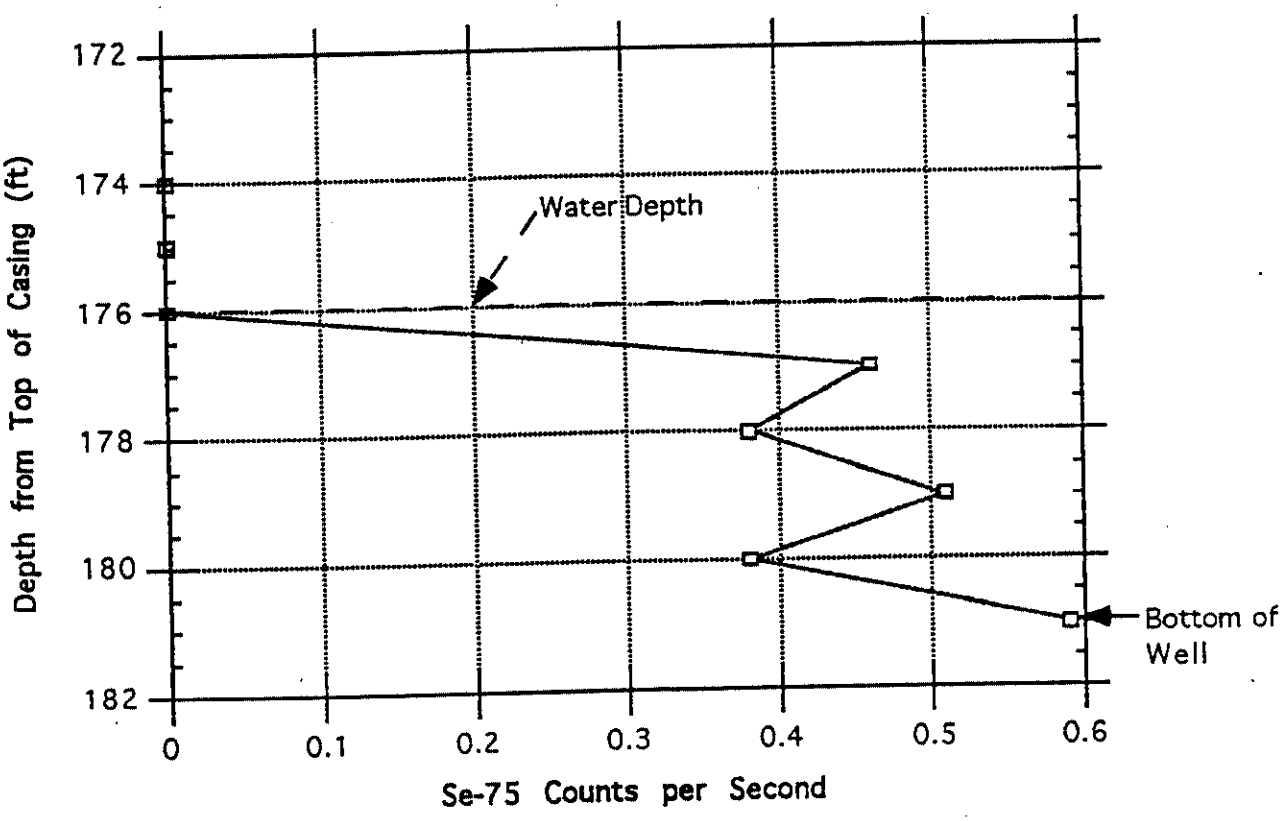

Figure 9. Selenium-75 counts per second vs. depth for the saturated zone of Well B12011 (NA).

Table 8. Gamma spectroscopy cross section data for Well B06N11 (GA) (data collected on August 30, 1994).

	Depth (ft)	Se-75 cps	C
1	174.00	0.0000	
2	175.00	0.0000	
3	176.00	0.22000	
4	176.50	0.43700	
5	177.00	0.41700	
6	177.50	0.53000	
7	178.00	0.48000	
8	179.00	0.53000	

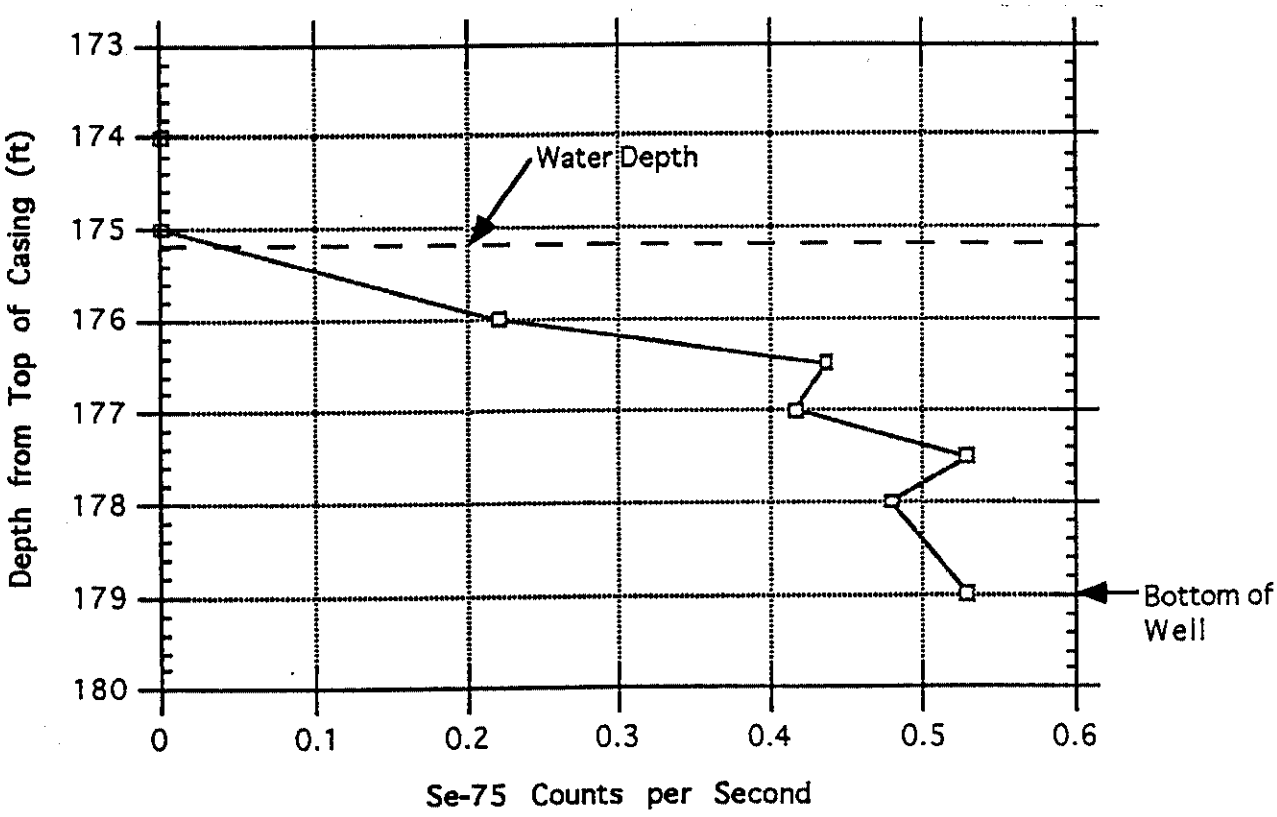

Figure 10. Selenium-75 counts per second vs. depth for the saturated zone of Well B06N11 (GA).

Table 9. Gamma spectroscopy cross section data for Well B04N11 (EF) (data collected on August 27, 1994).

	Depth (ft)	Se-75 cps	C
1	174.00	0.0000	
2	174.50	0.0000	
3	175.00	0.13000	
4	175.50	0.78000	
5	176.00	0.77000	
6	176.50	0.91000	
7	177.00	1.6300	
8	177.50	1.3600	
9	178.00	1.7100	
10	178.50	1.6200	
11	179.00	2.1100	
12	179.50	2.7400	
13	180.00	2.8300	
14	180.50	2.3500	
15	181.00	2.4800	
16	181.50	2.3100	
17	182.00	2.2300	
18	182.50	4.9200	

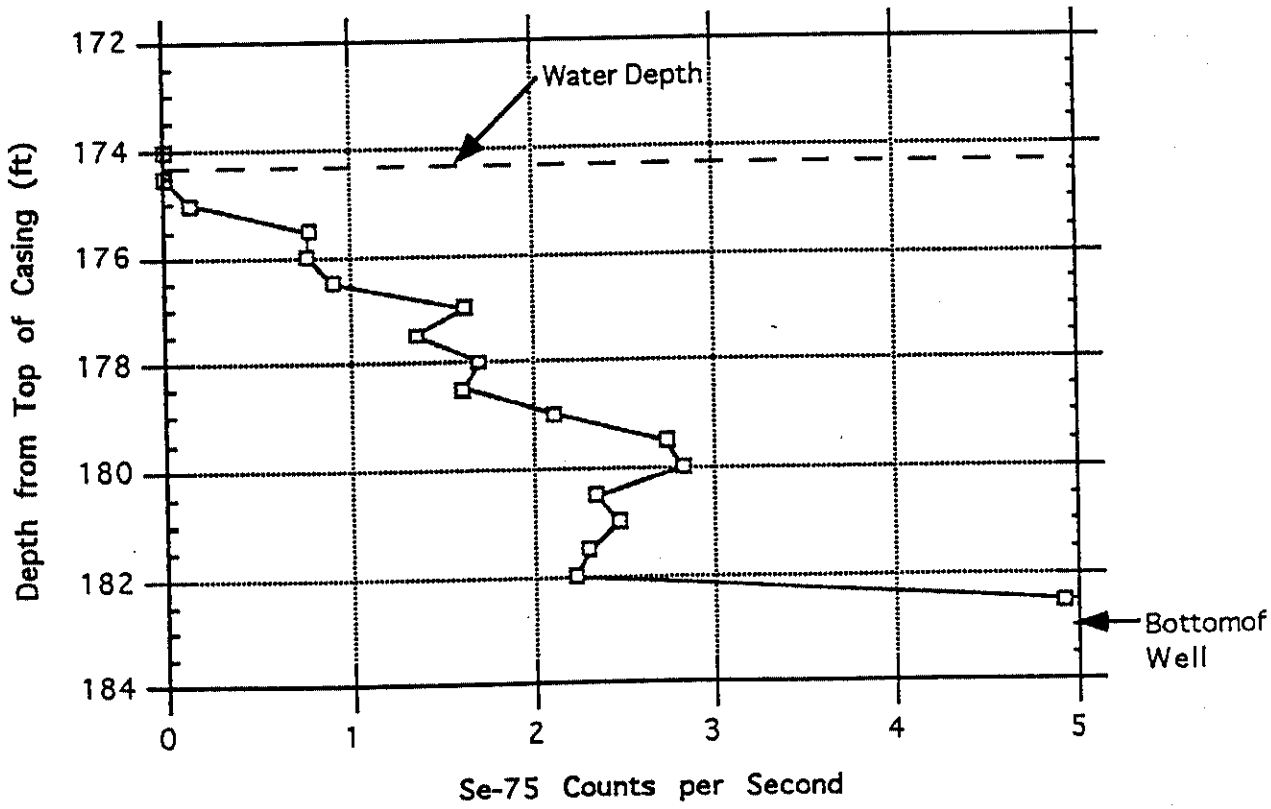

Figure 11. Selenium-75 counts per second vs. depth for the saturated zone of Well B04N11 (EF).

Table 10. Gamma spectroscopy cross section data for Well B08N11 (IF) (data collected on August 27, 1994).

	Depth (ft)	Se-75 cps	C
1	178.00	0.0000	
2	178.50	0.0000	
3	179.00	0.0000	
4	179.50	0.27000	
5	180.00	0.43000	
6	180.50	0.51000	
7	181.00	0.62000	
8	181.50	0.57000	
9	182.00	0.60000	
10	182.50	0.73000	
11	183.00	0.71000	
12	183.50	0.76000	
13	184.00	0.74000	
14	184.50	0.96000	
15	185.00	1.5000	
16	185.50	1.2100	
17	186.00	1.1900	

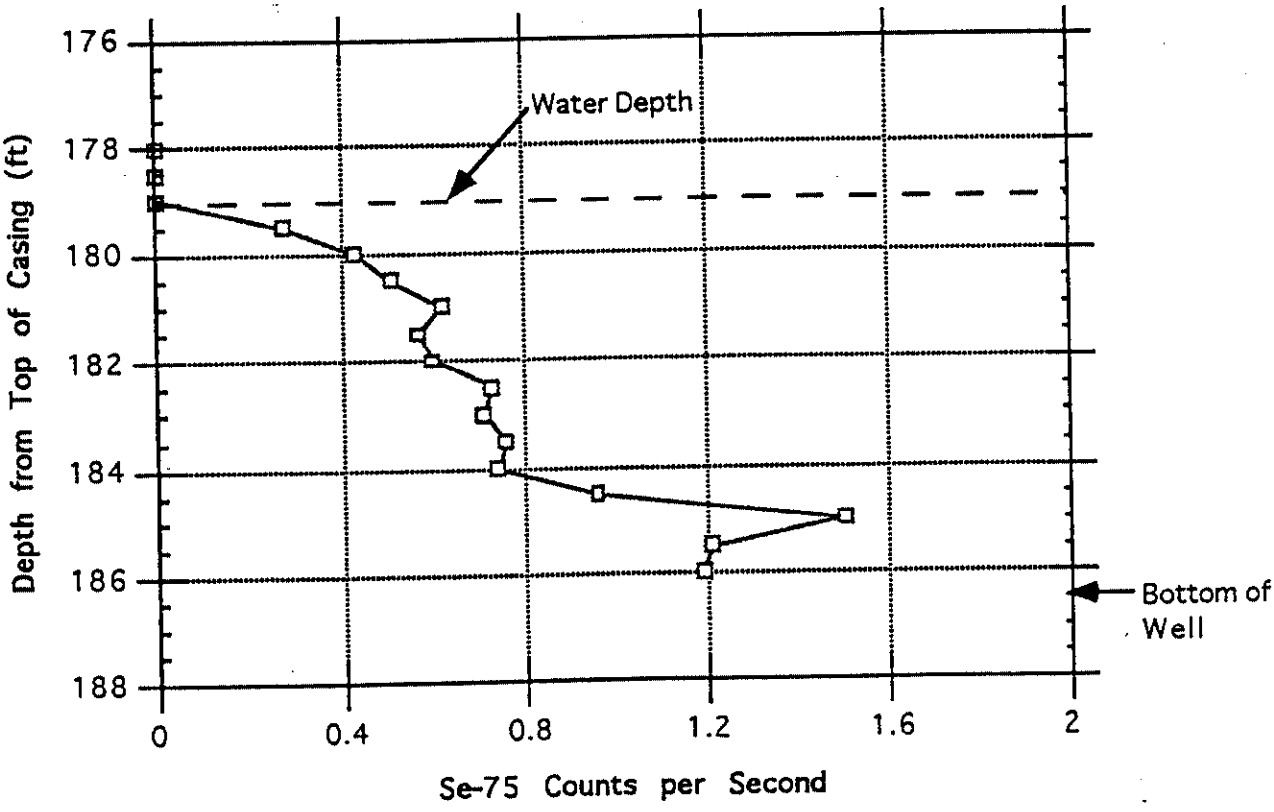

Figure 12. Selenium-75 counts per second vs. depth for the saturated zone of Well B08N11 (IF).

Table 11. Gamma spectroscopy cross section data for Well C04C11 (EG) (data collected on August 21, 1994).

	Depth (ft)	cps 21 Aug	cps 28 Aug	D
1	175.00	0.0000	0.0000	
2	175.50		0.0000	
3	176.00	0.0000	0.17000	
4	176.50		0.72000	
5	177.00	0.40000	1.6100	
6	177.50		1.4300	
7	178.00	0.79000	1.5600	
8	178.50		1.4400	
9	179.00	1.4200	1.8000	
10	179.50		1.7200	
11	180.00	1.6300	1.8200	
12	180.50		1.7800	
13	181.00	1.5400	1.6100	
14	181.50		2.6500	
15	182.00	2.2600	3.0200	
16	182.50		3.7400	

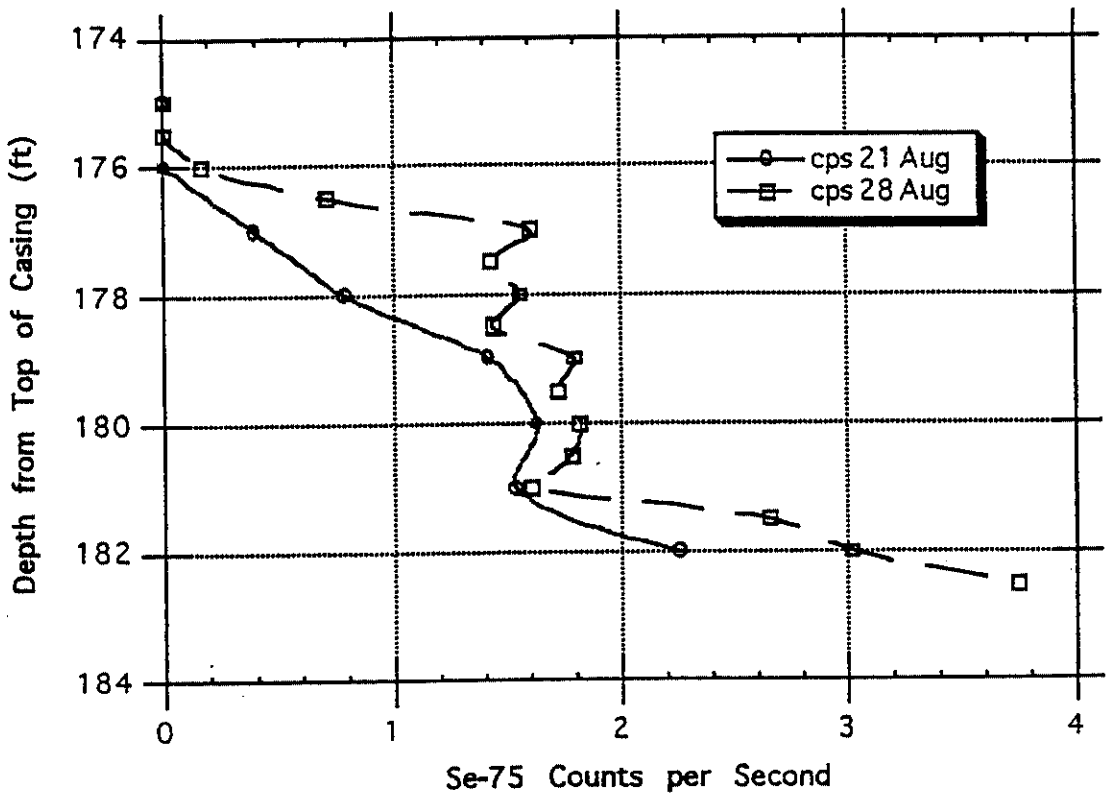

Figure 13. Selenium-75 counts per second vs. depth for the saturated zone of Well C04C11 (EG).

Table 12. Gamma spectroscopy cross section data for Well C02C11 (CB) (data collected on September 2, 1994).

	Depth (ft)	cps 28 Aug	cps 2 Sept	cps 6 Sept	cps 13 Sept	F
1	182.00		0.0000	0.0000	0.0000	
2	182.50					
3	183.00		0.0000	0.0000	0.0000	
4	183.50					
5	184.00		0.0000	0.24000	0.13000	
6	184.50					
7	185.00		0.35000	0.33000	0.39000	
8	185.50					
9	186.00	0.0000	0.42000	0.14000	0.58000	
10	186.50	0.0000				
11	187.00	0.37000	0.73000	0.46000	0.78000	
12	187.50	0.61000				
13	188.00	0.34000	0.81000	0.52000	0.80000	
14	188.50	0.49000				
15	189.00	0.34000	0.95000	0.49000		
16	189.50					

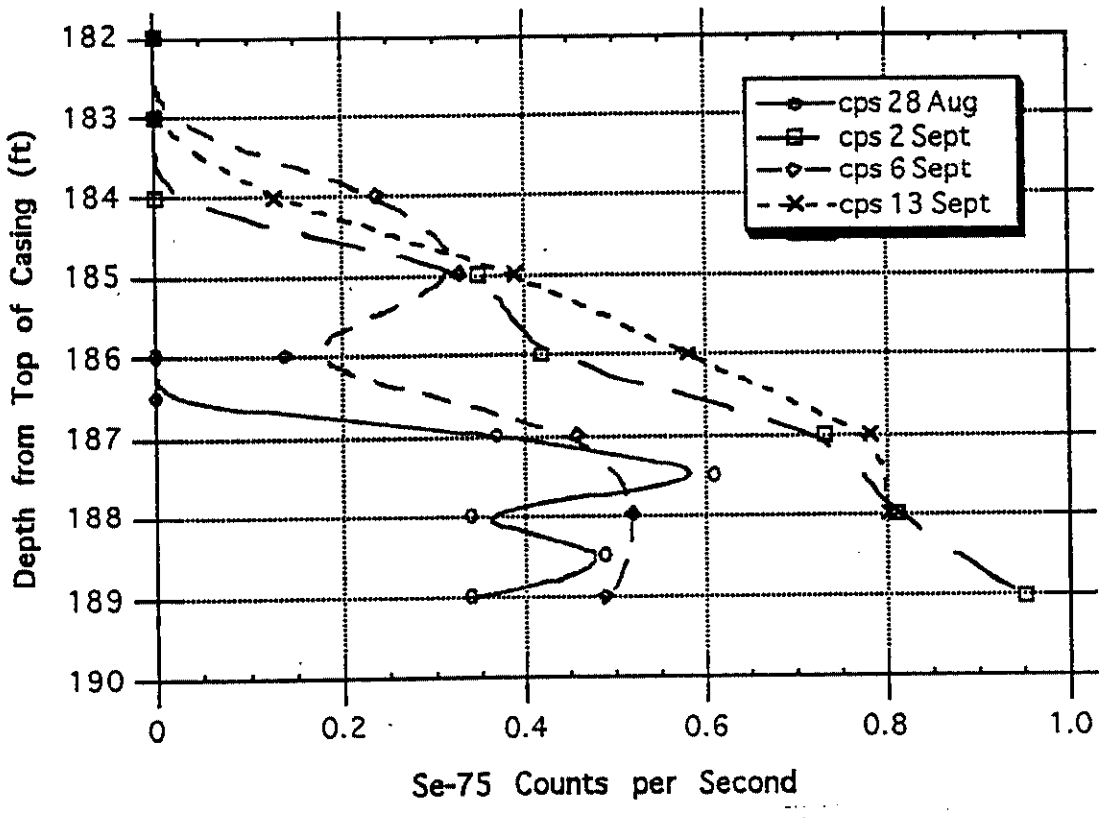

Figure 14. Selenium-75 counts per second vs. depth for the saturated zone of Well C02C11 (CB).

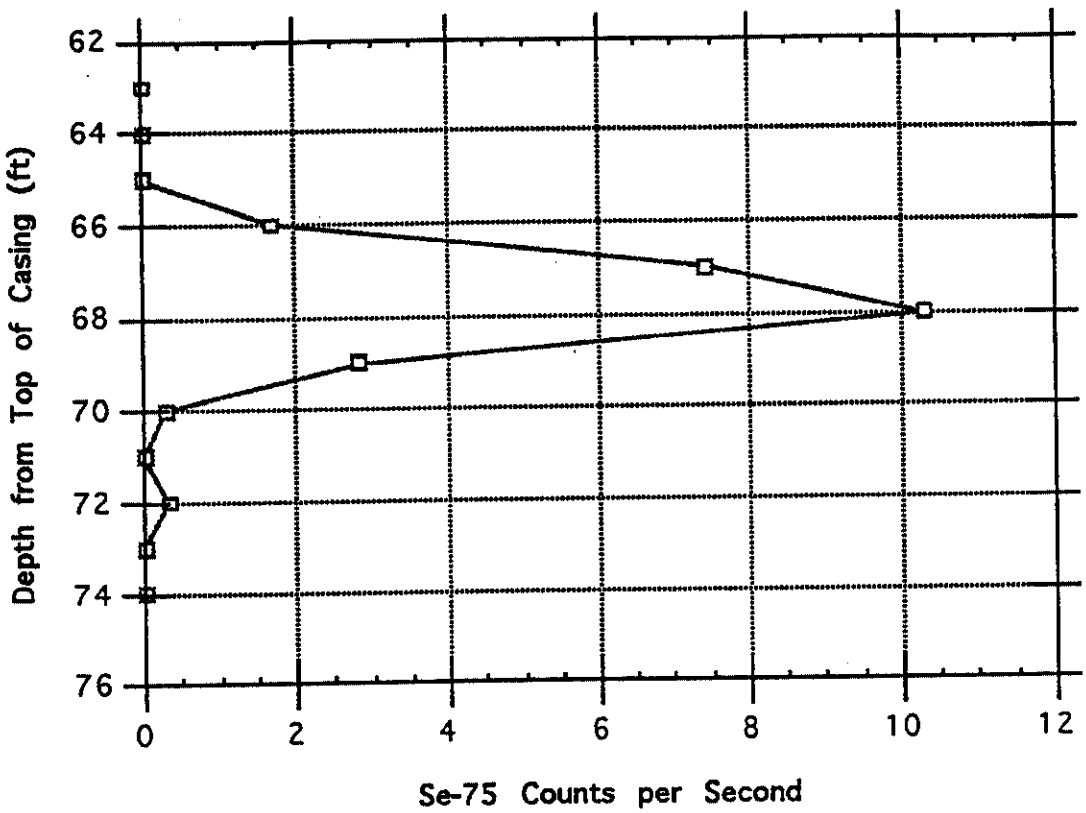

Figure 15. Selenium-75 counts per second vs. depth for the 62-76 ft zone of Well A11C12 (MD).

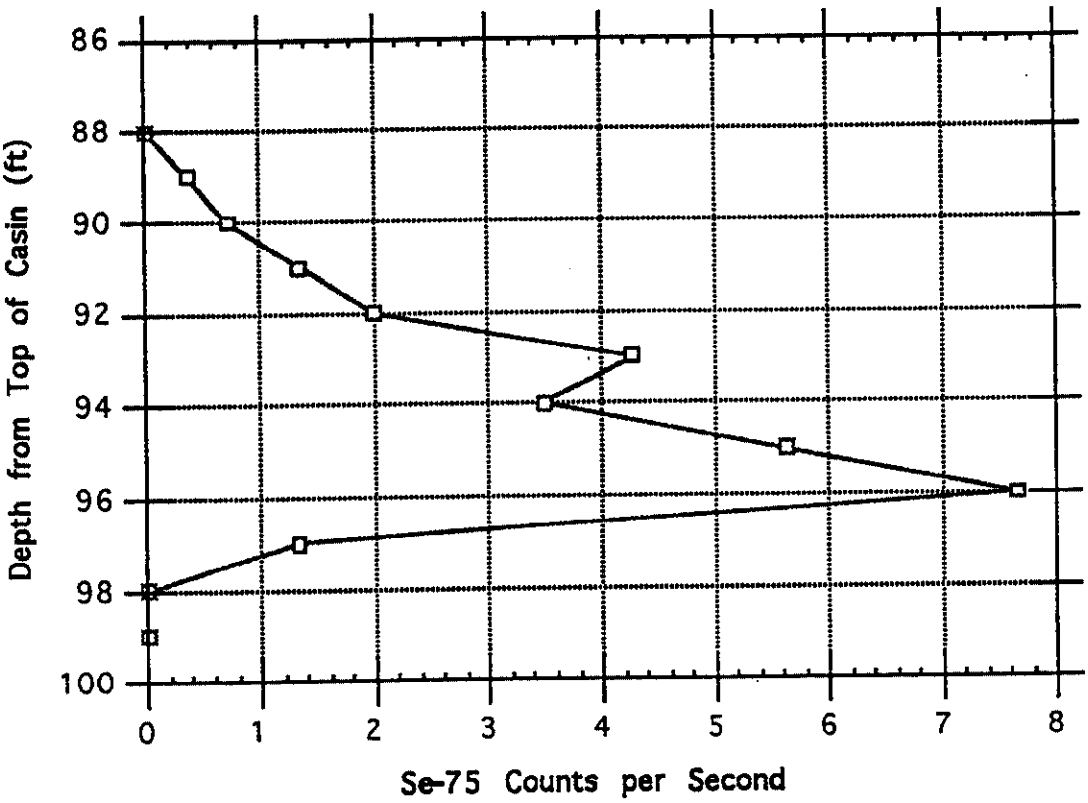

Figure 16. Selenium-75 counts per second vs. depth for the 86-100 ft zone of Well A11C12 (MD).

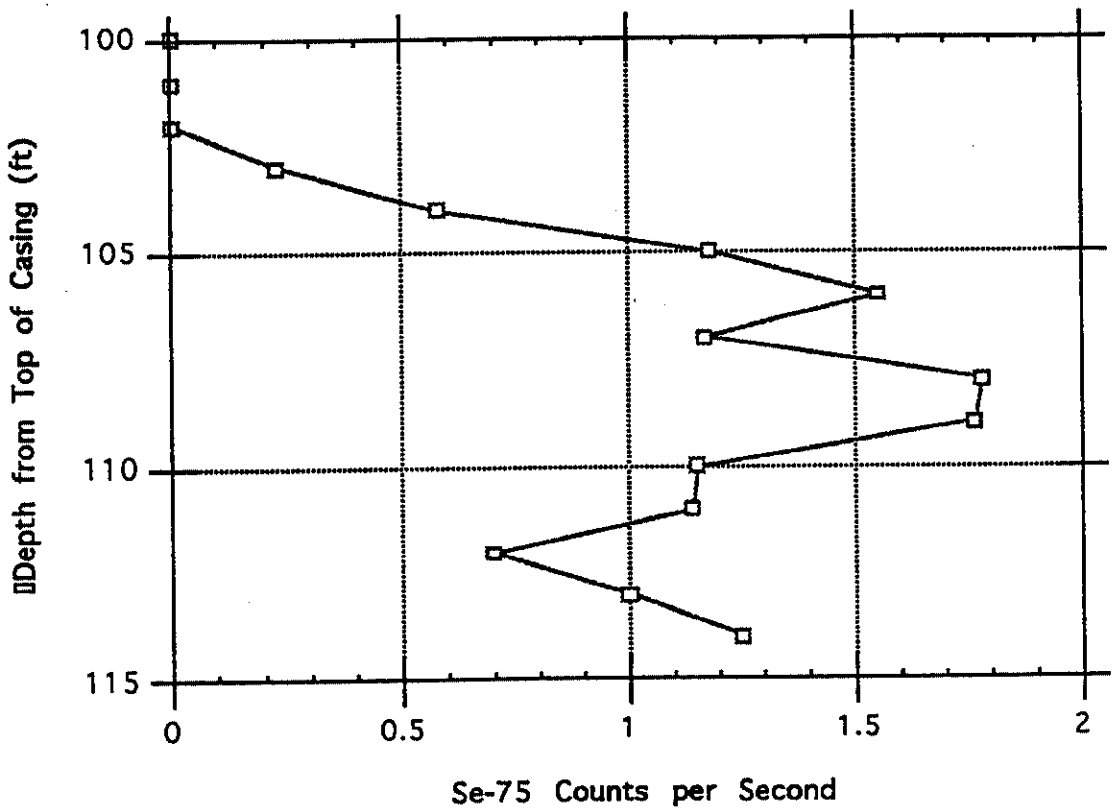

Figure 17. Selenium-75 counts per second vs. depth for the 100-115 ft zone of Well A11C12 (MD).

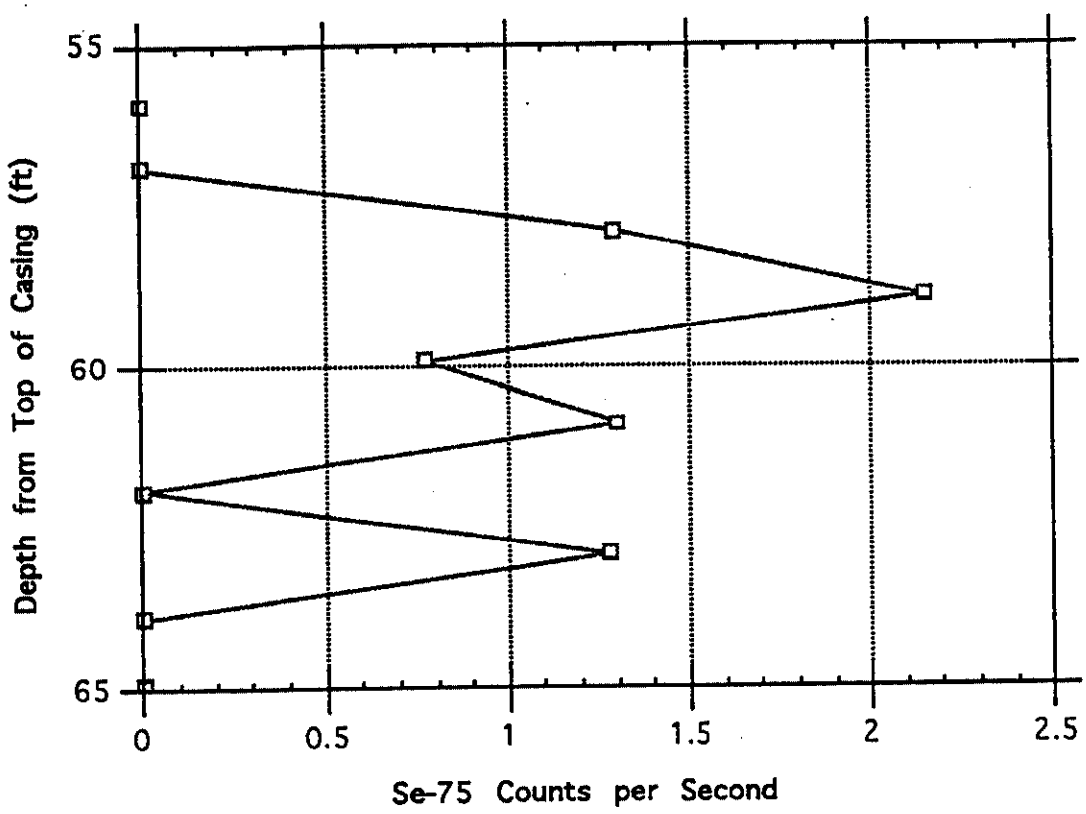

Figure 18. Selenium-75 counts per second vs. depth for the 55-65 ft zone of Well A01C11 (AB).

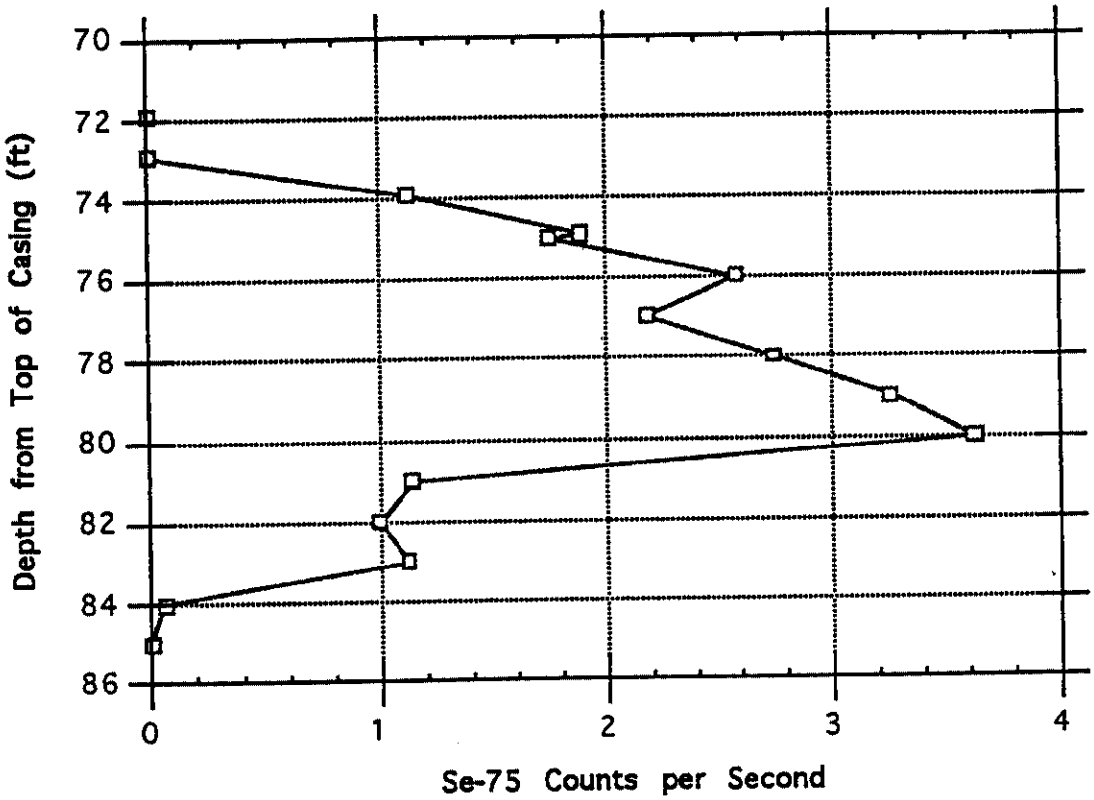

Figure 19. Selenium-75 counts per second vs. depth for the 70-86 ft zone of Well A01C11 (AB).

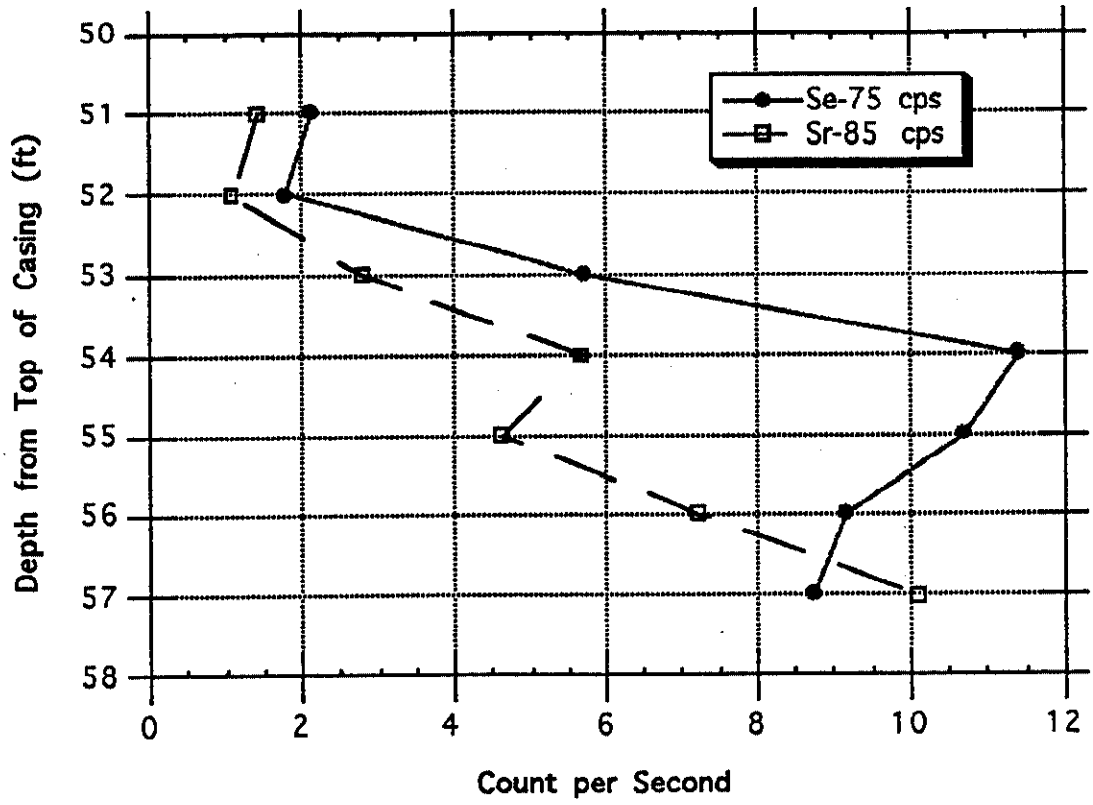

Figure 20. Selenium-75 and strontium counts per second vs. depth for the 51-57 ft zone of Well A11A31 (MA).

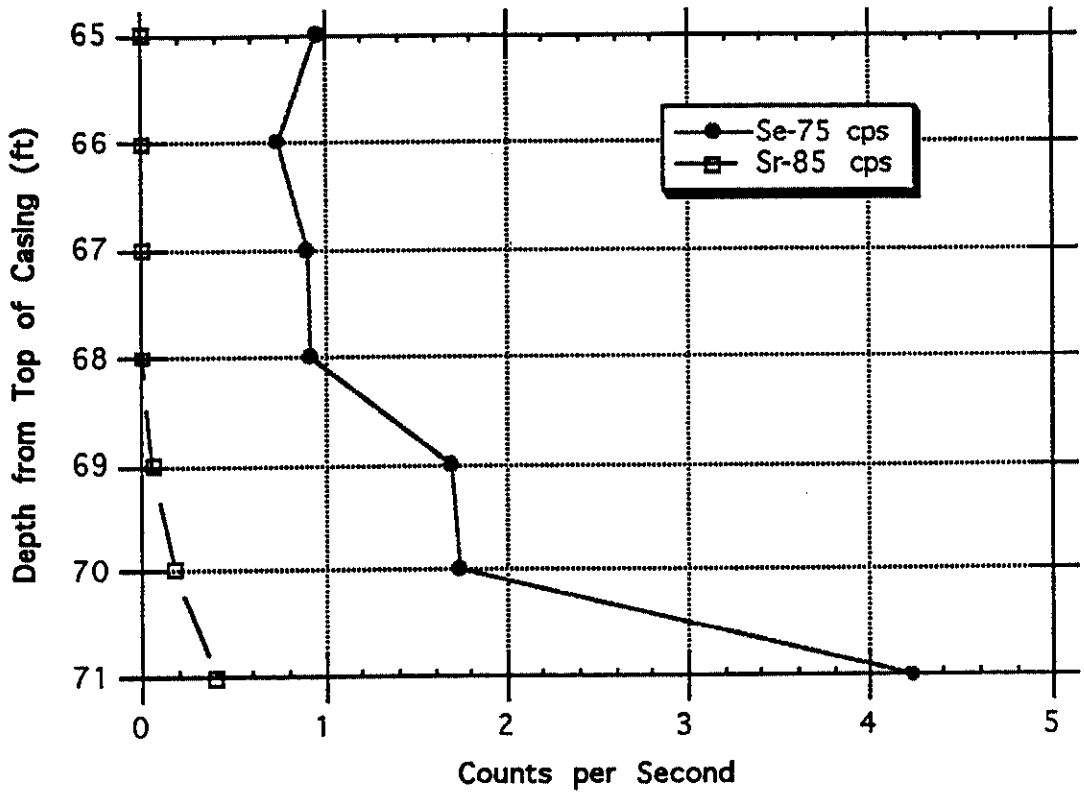

Figure 21. Selenium-75 and strontium counts per second vs. depth for the 65-71 ft zone of Well A11A31 (MA).